

# Safety System in Construction Industry

A protection system preventing fatal injuries by excavators in  
construction sites

Author:

Vo-Huynh, Quang-Nguyen

Helsinki Metropolia University of Applied Sciences

Bachelor Degree

Electronics Degree Programme

Bachelor Study

Date 16.12.2017

Author(s) Title  Number of Pages Date	Vo-Huynh Quang-Nguyen  Safety System in Construction Industry  53 pages + 3 Appendices 16 <sup>th</sup> December 2017
Degree	Bachelor of Engineering
Degree Programme	Electronics
Instructor(s)	Matti Fischer, Principal Lecturer Jani Virtenen, CEO of MDS Finland Oy
<p>The purpose of this study was the implementation of an automatic protection system for workers working near excavators, which is identified as one of the targeted hazards and causes for fatal injuries in construction sites.</p> <p>The automatic system consists of two key elements: the human presence detector based on the application of ultrasonic sensors and passive infrared sensors, and the active warning and alarm system based on the combination of audio and visual signalling devices, and wireless communication modules. On the other hand, the system also consists of several additional modules to enhance its performance. The system is planned to be installed on excavators for the detector part, and on the worker for the alarm and warning part.</p> <p>As such systems have not been utilized in the Finnish market. This system could optimistically become a common safety add-on in the Finnish and, if possible European construction industry, in the interest of accident prevention and limitation.</p> <p>Given that the time period for this study and research was limited, the targeted goal was limited to the successful implementation of one completed feature for this system, which is the ability to detect human presence, measure the distance between the workers and the excavator, and generate alarming message when the dangerous conditions are met.</p> <p>Overall, the target goal was managed to be achieved by presenting that the results of the measurement and evaluation of the system performance were completed. Following the conclusion of this study, further developments are needed to be conducted in order to be able to release a completed product to the market.</p>	
Keywords	Safety System, Construction Site, Occupational Healthcare

## Acknowledgements

Without the help from many great people involving both directly and indirectly, this study would have not been completed. Thus, the author would like to express a sincerest appreciation for their dedication and contribution for the completion of this work.

A special thank is given to Mr. Jani Virtanen -CEO of MDS Finland Oy, for endowing the author this heaven-sent opportunity to conceptualize and materialize the system. The author wishes to thank Mr. Matti Fisher, Mr. Janne Mäntykoski and Mr. Petri Valve -Senior Lecturers of Helsinki Metropolia University of Applied Science (UAS) and the supervisors and language guides of this study, for their patient guidance, technical support, invaluable plus constructive advice and critiques for this study work. The author is also particularly grateful for the assistance provided by Thanh-Thi Le – a junior Student from Helsinki Metropolia UAS, resulted in a detailed and throughout test for the sensors utilized in the system, which is one of the critical phases of the system development.

## Table of Contents

1	Introduction	1
2	Overview of Excavators	2
2.1	The Configurations of Excavators	2
2.2	Safety Performance Analysis of excavator	4
3	Theoretical Background about Sensors in the System	8
3.1	Overview of Sensors and Sensor Fabrications	8
3.2	Distance Measurement Sensors based on Ultrasonic Energy	11
3.3	Occupancy and Motion Detection Sensors Based on PIR Sensor	14
3.4	Velocity and Acceleration Sensors	18
4	Theoretical Backgrounds about the Communication Protocol	20
4.1	Overview of the Wireless Communication Protocol	20
4.2	Overview of ZigBee Technology	21
5	Development of the System	26
5.1	Methods and Resources	26
5.2	Overview of the System	27
6	Performance Test & Evaluation	32
6.1	First Prototype Performance Test	32
6.1.1	Test Procedure	32
6.1.2	Performance Results of the Ultrasonic Sensors	33
6.2	Second Prototype Performance Test	36
6.2.1	Test Procedure	36
6.2.2	Performance Test Results of PIR Sensors	39
6.2.3	Performance Test Results of the Power Monitor Module	41
6.2.4	Performance Test Results of the new Ultrasonic Sensors	46
7	Conclusions and Discussions	51
	References	52
	Appendix A	i
	Appendix B	iv
	Appendix C	viii

## List of Tables, Figures and Illustrations

Figure 1: Layout diagram of a standard construction excavator.

Figure 2: Performance Level Analysis of Excavators based on ISO 13849-1:2006.

Figure 3: The blind spots of excavators.

Figure 4: Operating principles of piezoelectricity effect.

Figure 5: Various possible vibration modes in piezoelectric ceramic materials.

Figure 6: Ultrasonic distance measurement operation principle.

Figure 7: Impedance characteristic of a piezoelectric sensor in single or multi layers.

Figure 8: The electromagnetic spectrum diagram.

Figure 9: A simplified model of pyroelectric effect.

Figure 10: Dual pyroelectric sensor

Figure 11: Optical lens in PIR sensor technology.

Figure 12: Piezoelectric accelerometer.

Figure 13: Three supported network topologies of ZigBee.

Figure 14: Product Breakdown Structure (PBS) for the Safety System.

Figure 15: Block diagram of the first prototype.

Figure 16: Block diagram of the Transceiver in the second prototype.

Figure 17: Block diagram of the Receiver in the second prototype.

Figure 18: The Test Site Layout for HC-SR04.

Figure 19: Drawbacks of the HC-SR04 sensor based on its performance test results.

Figure 20: Test Site Layout of the PIR sensor.

Figure 21: Arduino-to-Arduino Communication Setup for Sensor Performance Test.

Figure 22: Performance Limitation of Open PIR Sensor.

Figure 23: The schematic of the power monitor module.

Figure 24: Realization of the power monitor module in schematic format.

Figure 25: Realization of the power monitor module in the layout format for PCB manufacturing.

Figure 26: Performance measurement results of the power monitor module.

Figure 27: Performance measurement results of the HRLV-EZ0 sensor.

Figure 28: Different supply voltage value than the recommended one in HRLV-EZ0 leads to inaccurate distance measurement.

Figure 29: The shunt reference application circuit (left), and the general setup of the application to the Arduino microcontroller (right).

Table 1: Analysis of accident cases from Appendix A caused by excavators.

Table 2: The Open System Interconnection (OSI) Model.

Table 3: The main difference between ZigBee and Wi-Fi technology.

Table 4: Highlight features of the HC-SR04 features

Table 5: List of the main benefits and drawbacks of the two candidates for new ultrasonic sensor.

Table 6: Highlight features of the Open PIR sensor.

Table 7: Performance results of PIR sensor in indoor environment.

Table 8: Performance Results of the Open PIR sensor in the outdoor environment.

Table 9: Comparison between the Conventional Buck-Boost and the Micro DC-DC Converters.

## List of Abbreviations and Symbols

SIL	Safety Integrity Level
DNA	Deoxyribonucleic Acid
PMN-PT	Lead Magnesium Niobate-Lead Titanate
PIR	Passive Infrared
DC&CN	Data Communication and Computer Network
OSI	Open System Interconnection
WLAN	Wireless Local Area Network
WPAN	Wireless Personal Area Network
WSN	Wireless Sensor Network
TCP	Transmission Control Protocol
UDP	User Datagram Protocol
API	Application Program Interface
MAC	Media Access Control
PAN ID	Personal Area Network ID
EPID	Extended PAN ID
ACK	Network Acknowledgement
PBS	Product Breakdown Structure
OUT	Object under Test
LOS	Line of Sight
EUT	Equipment under Test
PUT	Person under Test

IEC 61508 (Functional safety of electronic safety-related systems)  
IEC 61511 (Safety instrumented systems for the process industry sector)  
IEC 62061 (Safety of machinery)  
ISO 13849-1:2015 (Safety of machinery: Safety-related parts of control systems)  
IEEE 802.11 (Technical Standard for Wireless Local Area Network Specification)  
IEEE 802.15 (Technical Standard for Wireless Personal Area Network)  
IEEE 802.15.4 (Technical Standard for Low-Rated WPAN)

## 1 Introduction

Occupational Healthcare has played a crucial role in the current society as a functioning methodology to promote a safe and healthy work environment. In Finland, this subject is one of the pioneered disciplinarians as issued by the Finnish Ministry of Social Affairs and Health to cope with the country's highly industrialized economy.

According to the statistics provided by the Finnish Institute of Occupational Healthcare and KELA –Finnish Social Welfare Agency, construction is among the key industries constituting a high percentage of work-related accidents and injuries. As a results, many regulations and rules are introduced to prevent and limit the likelihood of accident occurrence. Nevertheless, there are several issues which are overlooked, and this study is aiming to pinpoint one of those: the near non-existent provision of safety system for workers working near excavators.

Before entering the detailed report of the safety system, a general understanding about the excavator and the potential hazards it could cause is necessary to acquire. For this end, this work provides readers all the above information, plus the general safety analysis of the excavator, in the first chapter. Moving to the next two chapters, the work provides a theoretical background of the system by introducing the sensors integrated in this system and the employed communication protocol based on several distinguishing aspects, in order to pinpoint the main reasons for selecting those sensors and the current protocol.

In the fifth chapter, the prototypes of the system, their overviewed development process and their specifications are presented. The measurement results of these prototypes are presented for the evaluation and comparison phase in the sixth chapter.

In the final chapter, conclusions are reached based on the evaluation of the measurement results from the previous chapter, together with the general assessment of every development stage. This chapter also includes a discussion about the future of the system development.



## 2 Overview of Excavators

This chapter provides a brief introduction about the construction excavators in these following aspects: their common configurations, and their safety performance study. The latter aspect is the most important subject as it dictates the reason and the predicted requirements for the implementation of the targeted safety system.

### 2.1 The Configurations of Excavators

Excavators are heavy construction equipment, especially designed for mainly earthwork operations and other duties, such as moving large objects. Thanks to the devices, several tasks in construction industry now can be accomplished with a great reduce in manpower.

The standard excavator consists of six main parts, which are illustrated from right to left in Figure 1 below:

- An engine/counterweight, which is commonly configured as a diesel one, along with the hydraulic system controlling the boom and its attachment powers the excavator's undercarriage.
- A cab on a rotation platform, which is called the house, is stationed on top of an undercarriage with tracks and wheels. This compartment is where the operator controls the machine, and it rotates independently of the undercarriage thanks to the rotation platform.
- An undercarriage consisting smaller parts such as idler, tracks, rollers and drive sprocket is the bottom part of the excavator, underneath the cab.
- A boom, also called as a backhoe or rear reactor, is basically a long arm of the excavator, which connects one end to the main chassis (the cab and other compartments) and the other end to a joint (the elbow), and the stick holding the attachment.
- A dipper, or stick.
- An attachment, which is varied depending on the task the machine is configured to perform. The standard one has a bucket (a scoop) with toothed edge designed for bulk material handling.

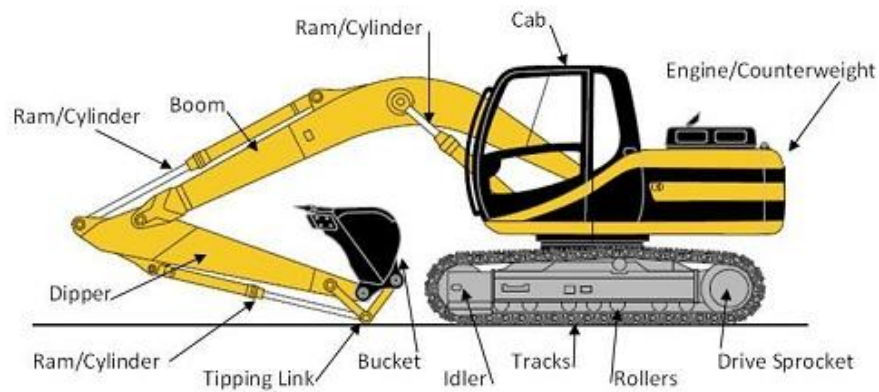


Figure 1: Layout diagram of a standard construction excavator (Source: HSE Professionals-Excavator Use & Safety Precaution).

Excavators come in a wide variety of sizes, which depend on the tasks they are configured to perform as mentioned above. The smaller ones are called compact excavators, the larger ones for example are dragline excavators used in civil engineering and surface mining for crane lifting, or long-reach excavators mainly used in demolition-related tasks in tall-stories buildings. Therefore, a separate study about dimensions of different construction excavators from endorsed vendors in the Finnish market should be conducted in order to establish an appropriate safety perimeter. Nonetheless, each construction supervisor should establish a suitable perimeter to suit the construction site that is currently under operation since each site has an enormous variety of area dimension, which properly renders the proposed range resulted by the study unfit to apply.

For easy testing purposes of this system, the safety distance between a worker and the excavator is currently set to be four meters, and the danger perimeter is set to be two meter.

## 2.2 Safety Performance Analysis of excavator

Similar to other industrial machines and equipment, excavator operation requires a strict and by-the-book training and supervision in order to control the risks.

Conventionally, it is required that all of the workers must participate in the safety training, and the area surrounding the excavators are properly marked with safety symbols, in order to minimize the frequency of accident occurrence. According to the HSE Training Manual (HSG 150), there are five main precautions necessary to control the hazards, usually abbreviated together as ECVSB:

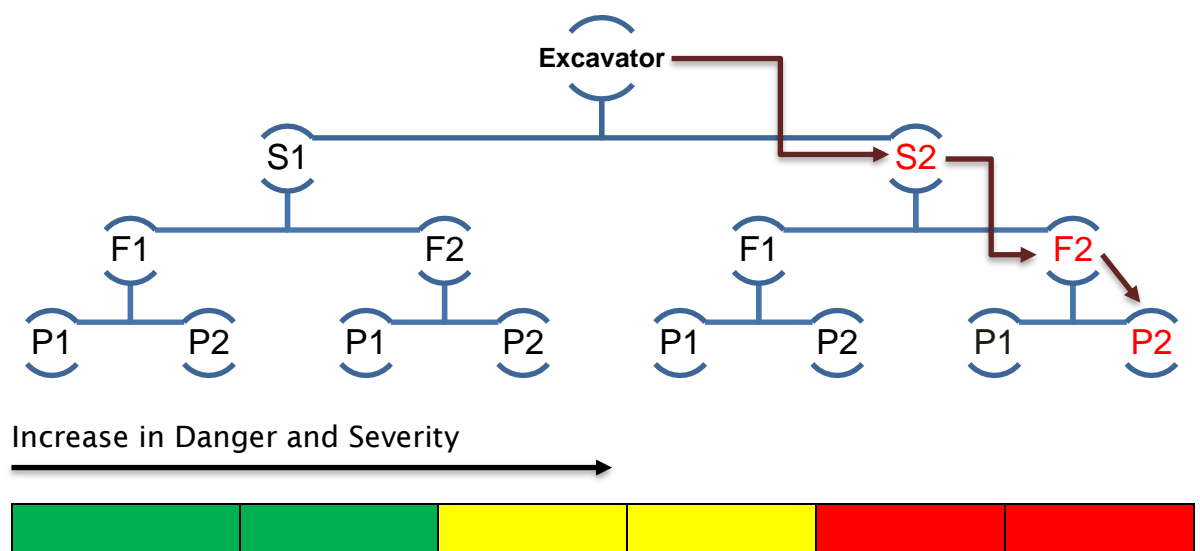
1. Exclusion: keeping people away by the provision of suitable barriers.
2. Clearance: a suitable clearance is preferred and maintained between any parts of the excavator and the nearest obstruction.
3. Visibility: excavators should be designed and equipped with adequate visibility to ensure operators can see areas where people may be at risk.
4. Signaler: there must be a signaler who is always located in a safe location to direct any excavator operation and pedestrian movement.
5. Bucket attachment: before the operation, bucket must be checked in order to ensure its secure during and after the operation; additionally, quick hitches can be used to secure the bicker to the excavator.

Thus, Finland is regarded as one of the countries with lowest number of occupational accidents in the construction industry per year due to the country's solid compliance to safety rules and regulations. Nevertheless, giving to the accounts that mishaps still occur, a robust and reliable safety system installed to excavators would be a sensible solution to further limit and prevent misfortunate incidents. In order to design such a system, it is imperative that a study about accident cases caused by excavator utilizations must be conducted.

Thanks to the cooperation with the Finnish Institute of Occupational Healthcare and the Finnish Worker's Compensation Centre, it was possible to receive a list of the accident cases to conduct his study. A brief analysis for these accidents is provided in Table 1, and Figure 2 below. The accident case list is included in Appendix A for possible further inquiry.

Table 1: Analysis of accident cases from Appendix A caused by excavators.

Types of Accidents	Injury method	Number of cases	Fatality result
Resulted by movement of excavator (I)	Compressed.	19	Death or severe injured
Resulted by one or several tools of excavator (II)	Rotation parts.	11	Death or severe injured
Resulted by other problems	Compressed; Fallen down; etc.	16	Death or severe injured



Severity of injury S1: slight/non-fatal. S2: severe/irreversible or dead.
Frequency and exposure time to hazard F1: seldom/less often and/or exposure time is short. F2: frequent/continuous and/or exposure time is long.
Possibility of avoiding hazard or limiting time P1: possible under certain conditions. P2: rarely possible.

Figure 2: Performance Level Analysis of Excavators based on ISO 13849-1:2006.

The accident case list was provided from the database of Finnish Institute of Occupational Healthcare, and the performance of the excavator was analysis based on the layout of ISO 13849-1:2006, which indicates the ability of control system to perform a safety function under foreseeable conditions.

To sum up the accounts of the above case study, injuries resulting from excavators were severe and unlikely to avoid when the accidents occurred. The main causes are to occur when the excavator is:

1. Moving: during the movement, it may strike the nearby workers or the pedestrian happened to come across the construction site (if the site is confined to small area), especially while reversing (classified as Type I).
2. Slewing: the excavator can potentially trap a person between it and a fixed structure or vehicle (classified as Type I or Type II depends on the exact situation).
3. Working: when operating, its moving bucket or other attachments may strike nearby workers/pedestrians (classified as Type II), or when the bucket inadvertently falls from the excavator (classified as Type II or Type III).

Among all of the Type I and Type II accidents, there is a notable similarity: they all were the consequence of workers unintentionally or unexpectedly standing within the dangerous vicinity or in the blind spots/corners to the excavator, which is illustrated in Figure 3 below. Those unfortunate incidents usually rendered the excavator operators the ability to effectively enact the safety measures.

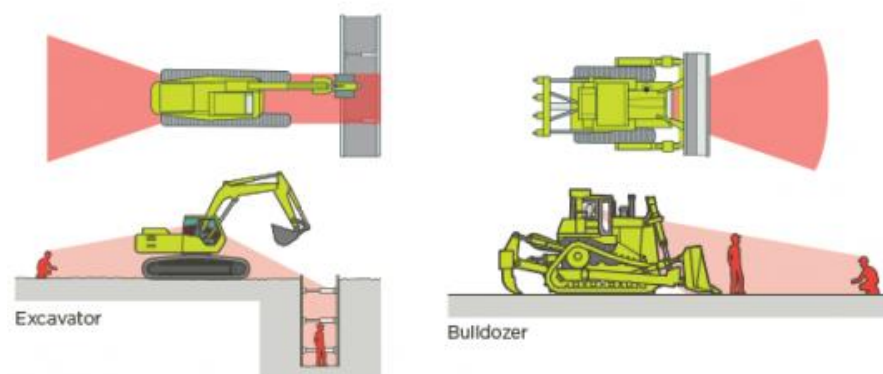


Figure 3: The blind spots of excavators (Source: Excavator Safety - WorkSafe New Zealand).

Following this study, it is determined that the safety system is recommended to be installed in the blind spots/corners. It is also recommended that the dimension study of the blind spots/corners should be conducted in order to deduct the appropriate number of sensors employed in each spot/corner to completely cover it. On the other hand, the system is required to be compliant with all of the associated safety standard regarded electronic safety-related systems in industry and machinery, which are the IEC 61508, the IEC 61511, and the IEC 62061.

### 3 Theoretical Background about Sensors in the System

This chapter provides a detailed key concepts of the integrated sensors in the system. Their performances are provided in the Measurement & Evaluation chapter.

#### 3.1 Overview of Sensors and Sensor Fabrications

Methods of sensor fabrication is numerous in many aspects, ranging from sensing materials to manufacturing technologies tailored for each particular use and design of every sensor (Fraden, Jacob 2004). In this work, the piezoelectric material which is common in sensor industry, is mainly concerned, since the majority of sensors implemented in this system are fabricated by this material.

A piezoelectric sensor is a sensor device utilizing the effect of piezoelectric phenomenon to measure the changes in pressure, temperature, strain and force applied to the material. The piezoelectric effect is the phenomenon, in which there is the accumulation of electric charge inside several materials such as bones, silicon impurities or DNA in human bodies in response to the applied mechanical pressure resulting by external force.

A brief explanation about the operating principle of this effect is given in Figure 4. Compared to other materials, the crystal (the regular and repeating atomic structure in a solid) in the piezoelectric material is unsymmetrical. Under normal conditions, these crystals are electrically neutral as, despite their unsymmetrical arrangement of atoms, all of the electrical charges in the atoms are perfectly balanced. When a mechanical stress occurs, this equilibrium is disturbed because of the structural deformation. The formation of electric dipole inside the material occurs, thus causing the net charge to appear.

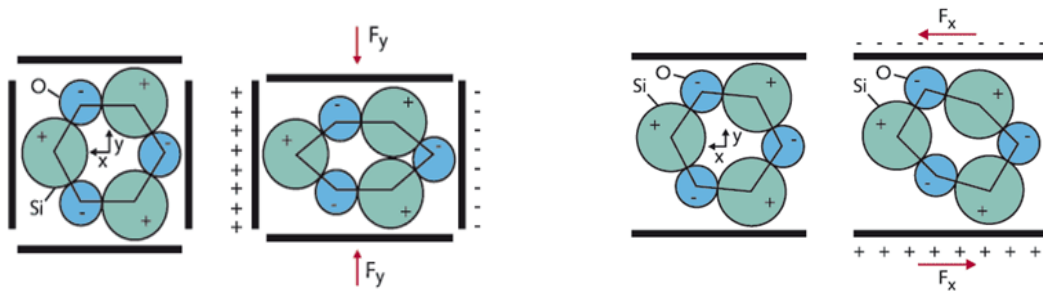


Figure 4: Operating principles of piezoelectricity effect (Source: How does a piezoelectric igniter work - Quora).

There are three key operating modes regarding the piezoelectric effect:

- Longitudinal mode: The amount of accumulating charge depends on the geometrical shape of the respective piezoelectric material.
- Transverse mode: The amount of displaced charges is strictly proportional to the mechanical pressure and is independent to the material size and shape.
- Shear mode: somewhat similar to the transverse operating mode, the amount of charges produced by this mode is proportional to the strength of the external applied force.

Materials used for piezoelectric sensors are divided into two main categories: the piezoelectric ceramic, and the single crystal materials. These materials bend. The material bends in many different ways correspond to the key operating modes above at different frequencies, meaning each material has a distinguish vibration mode.

- The ceramic materials have a significantly high piezoelectric constant, also known as sensitivity than those of the natural single crystal materials, and they can be produced by inexpensive processes. However, their high sensitivity degrades over time, plus this degradation is highly correlated with increased temperature.
- For the less-sensitive single-crystal materials, they have a higher to almost unlimited long term stability. With the introduction of new single-crystal materials now commercially available, such as Lead Magnesium Niobate-Lead Titanate (PMN-PT), these materials offer improved sensitivity compared to the ceramics', but they have a lower maximum operating temperature and are currently more expensive to manufacture.



The materials used to fabricate and manufacture sensors for our system comes mostly from the ceramic group. Since the performance of ceramic materials increasingly degrade with the increase in temperature, a good thermal management practice is required.

In Figure 5, different vibration modes and their working frequencies are presented. The implemented sensors for the safety feature involving the tasks of displacement measurement, occupancy-motion, and the acceleration sensor are operating in area and radius vibration modes.





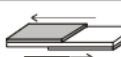

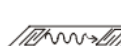

Vibration Mode		Frequency (Hz)								Application
		1K	10K	100K	1M	10M	100M	1G		
Flexure Vibration									Piezo Buzzer	
Lengthwise Vibration									KHz Filter	
Area Vibration									KHz Resonator	
Radius Vibration										
Thickness Shear Vibration									MHz Filter	
Thickness Trapped Vibration									MHz Resonator	
Surface Acoustic Wave									SAW Filter SAW Resonator	
BGS Wave									SH Trap SH Resonator SH Filter	

Figure 5: Various possible vibration modes in piezoelectric ceramic materials (Source: Handbook of Modern Sensor – Fraden, Jacob 2004).

### 3.2 Distance Measurement Sensors based on Ultrasonic Energy

The measurement of position and displacement of physical objects is essential for many applications: industrial controller systems, transportation traffic control, security systems, robotics, and especially safety evaluation, which is vital for occupational safety and healthcare practice. By determining the location (relative location in respect to a selected reference) and displacement (change of position from one to another in a specific distance or angle) of a person, it is possible to determine his or her distance to potential hazards in the current workplace environment to reduce the exposure chances as a mean to prevent accidents to happen.

For noncontact proximity distance measurement, an active sensor (a sensing device requiring external power sources to operate) capable of transmitting a pilot signal and receiving a reflected signal after being incident on an object can be used. This is the basis of ultrasonic sensor – a sensor popularly used as distance measurement and velocity detectors. This is one of the sensors utilized in this topic.

The working mechanism of ultrasonic sensors is, as hinted above, based on for the transmission and reception of ultrasonic energy from the homonymous waves. Ultrasonic waves are mechanical acoustic waves whose characteristics are like audible sound waves, except their frequencies cover the range well beyond the detectable capabilities of human ears (i.e., over 20kHz). Ultrasonic waves behave as longitudinal waves traveling along the direction of wave propagation through medium. Like any other mechanical or electromagnetic waves, when the ultrasonic waves are incident on an object, a part of their energy is reflected. The reflected waves are uniform in a solid wide range of angle regardless of the direction they are come from, and if the objects move, the reflected waves will have a different frequency than the transmitted waves due to the Doppler Effect (Fraden, Jacob 2004). On the other hand, the amplitude of reflected waves depends on many factors, such as: the amount of available incident surface; the size, shape and orientation of incident surface; and finally the material composition of the object.

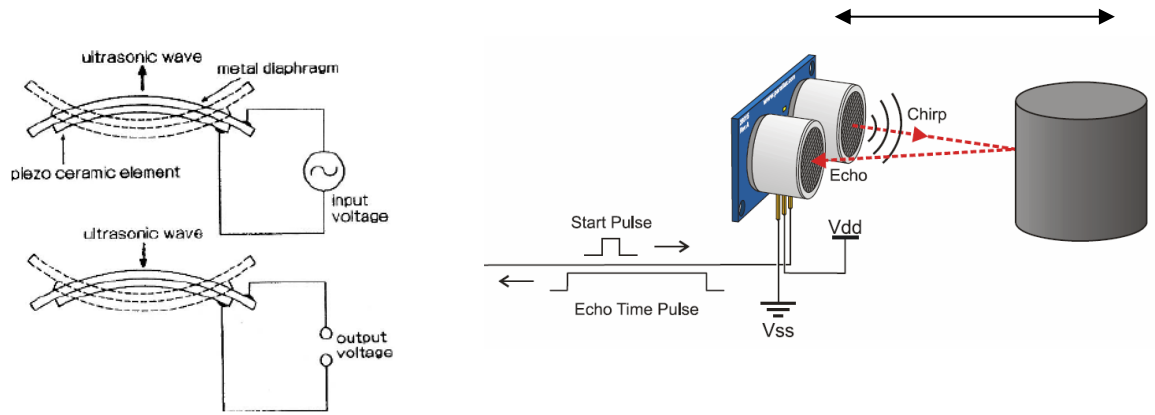


Figure 6: Ultrasonic distance measurement operation principle (Source: Handbook of Modern Sensors – Fraden, Jacob 2004).

The sensor operation is presented Figure 6: in the ultrasonic sensor, when the input voltage (Start Pulse) is applied to the ceramic element, the ceramic starts to flex and transmit ultrasonic bursts whose operating frequency is approximately around 40kHz. Because the piezoelectric effect is reversible, the ceramic in turn generates a voltage (Echo Time Pulse) when it is bended by incoming ultrasonic waves. During the transmission and reception of the sonic bursts, an integrated timer (stopwatch) is triggered at the exact moment when the bursts are transmitted, and stopped when the reflected bursts are received to measure the time length of the whole process. This timer has an increment of every few microsecond or even nanoseconds guarantying that measurement errors are limited to be miniscule.

The distance  $L_0$  to the object can be calculated through the speed  $v$  of the waves in the media, the transmitter and receiver relative position angle  $\theta$ , and the time for the ultrasonic waves to travel to the object and back to the receiver  $t$ :

$$L_0 = \frac{v \times t \times \cos \theta}{2} \quad (1)$$

If a transmitter and a receiver are positioned close to each other, then  $\cos \theta = 1$ .

With the speed of sound is 344m/s, from (1), the best expected resolution  $D$  for ordinary microcontrollers can be computed as:

$$D = \frac{v \times \Delta t \times \cos(\theta)}{2} = \frac{344 \times 10^{-6} \times 1}{2} = 0.000172 \text{ m} \quad (2)$$

In which  $\Delta t$  is the smallest time increment, assumed to be one millisecond.

By traveling with the speed of sound compared to the speed of light at which the electromagnetic waves propagate, the time is much longer and its measurement is easier and cheaper to be accomplished, hence the reason ultrasonic waves is favoured for distance and velocity measurement (Fraden, Jacob 2004).

It is noteworthy that driving oscillator resulting in the start pulse must be adjusted to generate a frequency equals to the resonant frequency  $f_r$  of the piezoelectric ceramic, where the sensitivity and the efficiency of this element is at best, as shown in Figure 7. There are other matters such as in the continuous transmission of ultrasonic waves systems, multiple layers of piezoelectric layers possessing higher sensitivities, as in Figure 7 are employed for both the transmitter and the receiver (Fraden, Jacob 2004), and ultrasonic transducers have the relatively narrow beam width.

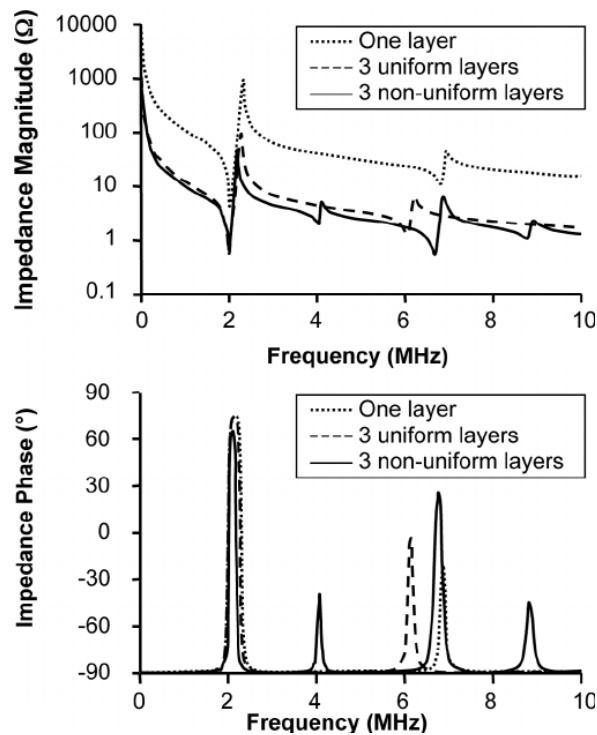


Figure 7: Impedance characteristic of a piezoelectric sensor in single or multi layers (Source: Mathematical Optimization of Multilayer Piezoelectric Devices with Nonuniform Layers by Simulated Annealing - Abrar, Aneela; Cochran, Sandy 2007).

To sum up, ultrasonic sensor efficiency relies majorly on the sensitivity of the ceramic layer(s). To select the most efficient and accurate sensor, these aspects are recommended to check before using the sensor:

- The frequency of the driving oscillator: as mentioned above, this frequency must match the resonant frequency of the ceramic layer(s).
- The resolution of the timer: the measured time length directly influences the accuracy of the resulted distance. Thus, the smaller the timer resolution, the smaller the resolution of the distance, hence the more accurate the result will be.
- The sensor beam width: the narrower the beam width, the more sensitive the transducer is. Though, it means there is a trade-off: more sensors are required to achieve a wide measuring angle.

### 3.3 Occupancy and Motion Detection Sensors Based on PIR Sensor

Continuous surveillance within a danger perimeter in the workplace environment is also one of the main considering tasks for occupational safety and healthcare. By detecting whether there is a person within the danger perimeter, it is possible to actively respond even before accidents happen, thus tremendously improving our performance in risk accidents prevention and limitation.

Presence readings are detectable by the utilization of occupancy or motion sensors. The occupancy sensors detect the presence of people or animals, and motion sensors detect the presence of moving objects within a monitored area. The main distinction between these two sensor types is that occupancy sensors produce data signals whenever an object is stationary or not, whereas the motion sensors are sensitive only to moving objects (Fraden, Jacob 2004). Depending on the applications, human presence can be determined by detecting the presence of several aspects of human body such as weight, heats, sounds, dielectric constants, et. or body action. In this study, Passive Infrared (PIR) sensor was used to for human presence detection, which is extremely popular in security and energy management system.

All objects, including human bodies, emit electromagnetic radiation, which is conventionally known as thermal radiation, whose wavelength depends on their

holding temperature. Most of the radiation emitted by human bodies lie within the infrared region, mainly at the wavelength of  $20\mu\text{m}$  –the “beyond the red” region located on the left side of the visible spectrum illustrated in Figure 8. The PIR sensing element inside the sensor is responsive to the far-infrared radiation, whose spectral range is from  $4\mu\text{m}$  to  $20\mu\text{m}$ , in order to detect human radiation, and this element is made of pyroelectrics, which are endorsed exclusively for the motion detector due to their simplicity, low cost, high responsivity, and broad dynamic range (Fraden, Jacob 2004).

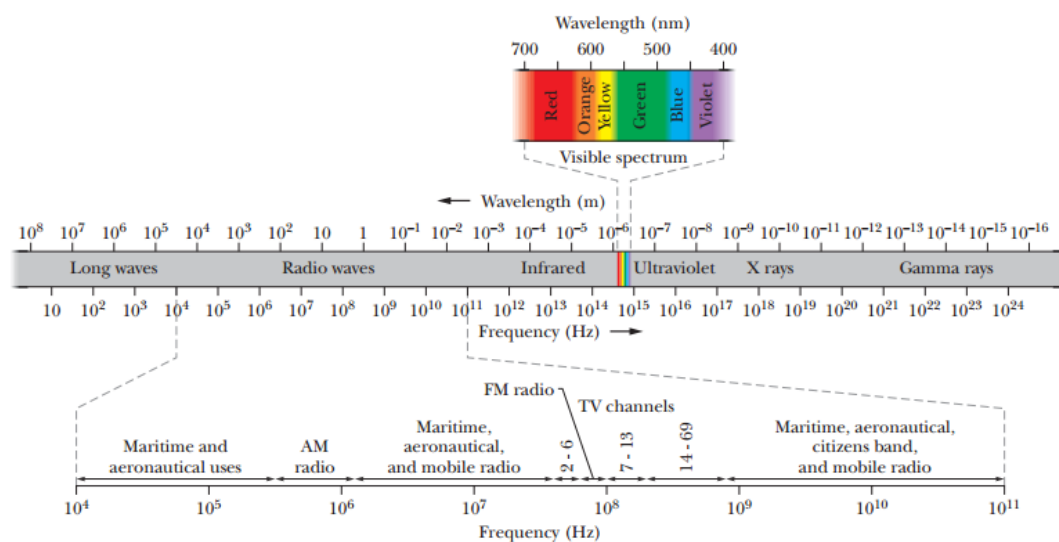


Figure 8: The electromagnetic spectrum diagram (Source: Fundamental of Physics – Halliday, David 2011).

A simplified operating principle is shown in Figure 9: a pyroelectric material generates an electric charge in response to the thermal energy flowing through its body thanks to the material thermal expansion. Similarly, like piezoelectric, pyroelectric materials upon absorbing heat causes its front side to expand, and generates a thermally induced stress and in turn generates a voltage. However, as a side effect, if a mechanical stress by external force induces to the sensing element, a voltage is also generated and in most cases, it is indistinguishable from the one caused by infrared radiation waves. Therefore, the pyroelectric sensor is usually fabricated in a symmetrical form by putting two identical elements inside the sensor's housing, which is called the dual pyroelectric model shown in Figure 10: a sensing element with a front/ upper electrode and two

bottom electrodes deposited on a common crystalline substrate. These elements are connected to the circuit in a manner so that they will produce the out-of-phase signals when subjected to the same in-phase inputs. If there are interferences due to the piezoelectric effect applied simultaneously, they will be cancelled at the input of the circuit. On the other hand, the to-be-detected thermal radiation will only be absorbed by only one element, thus avoiding the cancellation (Fraden, Jacob 2004).

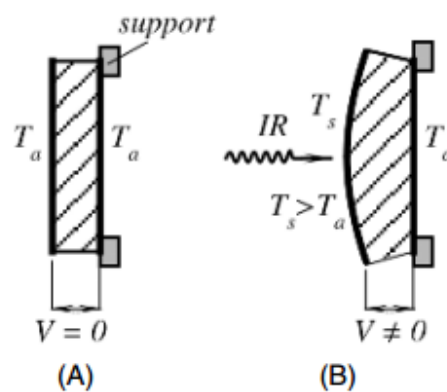


Figure 9: A simplified model of pyroelectric effect (Source: Handbook of Modern Sensors – Fraden, Jacob 2004).

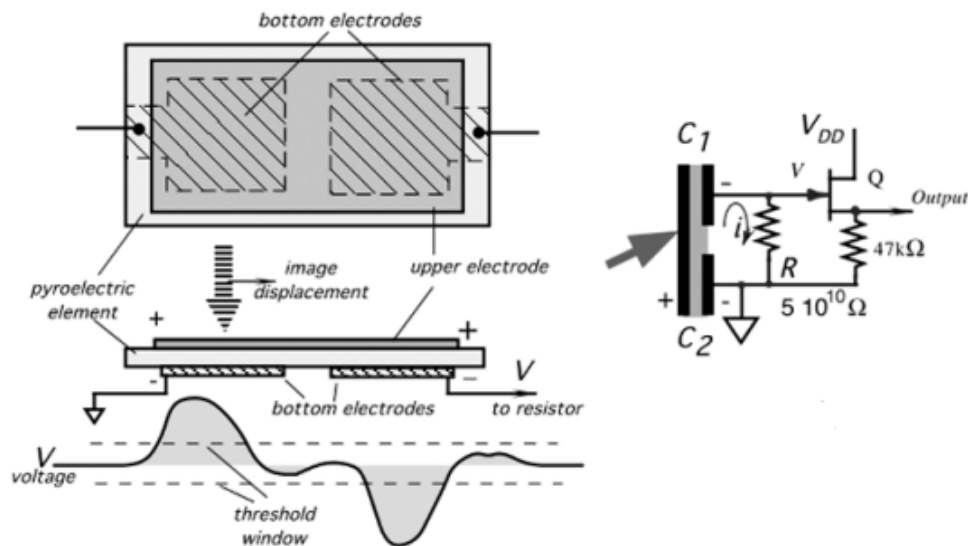


Figure 10: Dual pyroelectric sensor (Source: Handbook of Modern Sensors – Fraden, Jacob 2004)

The inserted optical device plays a significant role in PIR sensor technology. Thanks to the optical device, the received thermal radiation becomes focused into a miniature thermal image on the surface of the sensor. The energy from the image then is absorbed by the sensing element and converted into heat, which in turn is converted by the pyroelectric crystalline element into an electric current and voltage (Fraden, Jacob 2004). Thus, the optical device, which is made in the form of optical Fresnel lens, directly affects not only the signal magnitude but also the breath, range, and sensing patterns. Despite adding distortions, Fresnel lens condenses the thermal radiation providing a larger range of infrared to the sensors, as seen in Figure 11.

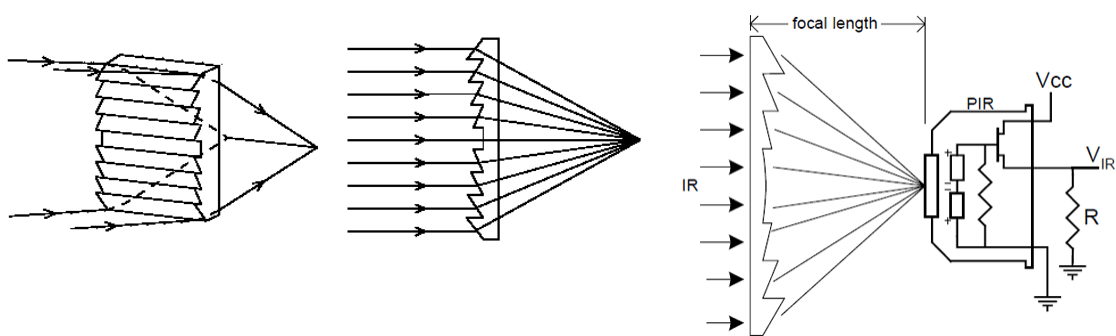


Figure 11: Optical lens in PIR sensor technology (Source: Handbook of Modern Sensors – Fraden, Jacob 2004).

For the conclusion, PIR sensor performance is based on the received amount of infrared power (flux). There are several factors contributing to the sensor performance and hence its efficiency, such as:

- The temperature difference (thermal contrast) between the object and its surroundings, which is also known as the ambient temperature. This issue is importantly addressed in the Measurement & Evaluation chapter.
- The surface area of the object which faces to the detector.
- The thickness of the sensing element: the thinner the element, the more sensitive is the detector.
- The material used to fabricate the lens, and the lens area.



### 3.4 Velocity and Acceleration Sensors

Considering a moving object, a compact way to describe its position during its motion is with a graph of its position  $x$  plotted as a function of time  $t$  – a graph of  $x(t)$  (Halliday, David 2014). From the function  $f = x(t)$ , two dynamic characteristics are derived: the first derivative – instantaneous velocity (commonly referred simply as velocity), and the second derivative – acceleration. Velocity determines the rate at which the position  $x$  is changing with a time at a given instant, and the acceleration, in turn, determines the rate of velocity change at this instant.

However, in real life measurement, the velocity and acceleration quantifiers are not derived from the position detectors but rather by special sensors. As a rule of thumb, in low frequency applications with a bandwidth on the order of 1 Hz, position and displacement measurements are generally used; on intermediate frequency ones, velocity measurement is favored, and acceleration measurements is preferred in measuring high frequency motions with appreciable noise levels (Fraden, Jacob 2004). In this study, the system is outfitted with accelerometer to measuring the motion of excavator arm as this sensor is able to sense both static (gravity), and dynamic (sudden starts and/or stops) acceleration.

Capacitive, piezo-resistive and piezoelectric displacement conversions are three of the proven and reliable methods, of which the latter is more popular. For the piezoelectric-type sensor, which was employed in the system, there are two major components inside an accelerometer, which are shown in the sensor layout in Figure 12 below: a special component usually called either a seismic or an inertial mass whose movements lags behind that of the accelerometer housing, and a displacement transducer employed to generate an electrical signal if it detects the mass displacement of this component in the form of measuring the resulted voltage with respect to the accelerometer housing as a proof of the acceleration. Therefore, any transducer capable of measuring microscopic movements under vibrations are suitable to use in the accelerometer. The value of the acceleration is derived based on Newton's Second Law of Motion, in which  $F$  is the displacement and  $M$  is the mass of the seismic component:

$$F = M \times a. (3)$$

This sensor possesses a wide bandwidth from as low as 2Hz to as high as 5kHz, good off-axis noise rejection, high linearity, and a wide operating temperature range (up to 120°C). For good frequency characteristics, a piezoelectric signal is amplified by a charge-to-voltage or current-to-voltage converter (Fraden, Jacob 2004).

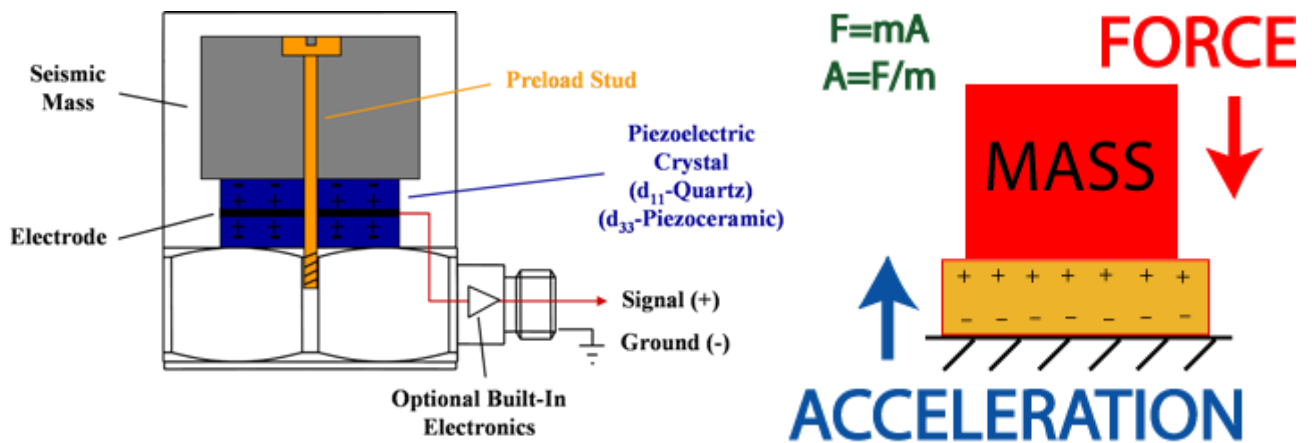


Figure 12: Piezoelectric accelerometer (Source: Accelerometer - Sparkfun).

#### 4 Theoretical Backgrounds about the Communication Protocol

This chapter provides a detailed information about the communication protocol, mainly the employed protocol in the system of this study.

##### 4.1 Overview of the Wireless Communication Protocol

Communication Protocol involves mainly the process of Data Communication and Computer Network (DC&CN). This process is described by the Open System Interconnection (OSI) model, which is presented in Table 2.

Table 2: The Open System Interconnection (OSI) Model.

OSI Model			
	Layer	Protocol Data Unit	Function
Media Layers	1. Physical	Bit	Transmission and reception of raw bit streams
	2. Data Link	Frame	Reliable transmission of data frames between two nodes connected by a physical layer
	3. Network	Packet	Multiple-node network management and structuring
Host Layers	4. Transport	Segment (TCP) Datagram (UDP)	Reliable transmission of data segments between points on a network
	5. Session	Data	Communication session management
	6. Presentation		Translation of data between a networking service and an application
	7. Application		High-level application program interface (API)

Because the Wireless Communication is used in this work, it is clearly from the OSI model that the main focus for the protocol establishment relies in the media layers.

As its name implies, this communication basically relies on the implementation of Wireless Transmission, which is a form of unguided media exchange involving no physical medium between two or more devices. Electromagnetic wave at radio and microwave frequency ranges serves as the basis and also the most endorsed medium for this transmission thanks to its beneficial properties: it is easy to generate given our current modern technologies; it is easy to penetrate through walls or similar structures; it has a diverse transmission depending on its frequency – lower frequencies mean longer range, up to 100,000km; and it can send and/or receive data with high speed.

In this study, only the wireless network within a limited area is concerned, also known as wireless local area network (WLAN), and the wireless personal area network (WPAN) based on IEEE 802.11 and IEEE 802.15 respectively. Two of the most common wireless networks belonged to the above groups and widely used in wireless sensor network technologies (WSN) are Wifi, and ZigBee, of which the latter is included in this study based on its beneficial properties explained below.

#### 4.2 Overview of ZigBee Technology

There are three main factors to consider, which are power, bit rate, and range when choosing which wireless network technologies to implement the sensor network. The Table 3 below informs about the main comparison between ZigBee and Wi-Fi, and proves why ZigBee is more suitable than its counterpart in this study.

Table 3: The main difference between ZigBee and Wi-Fi technology.

	Wi-Fi	ZigBee
Power	-High Power Consumption -Battery Life: several days	-Low Power Consumption -Battery Life: several years
Bit Rate	-High Bit Rate -Maximum bit rate: up to 54 Mb/s	-Low Bit rate -Maximum bit rate: 250 kB/s
Range	Maximum range: ~100 m	Maximum range: ~ 1000 m

ZigBee is the interconnection network for wireless sensing nodes requiring low power consumption without neglecting and sacrificing the reliability and the sustainability of the network itself. As the network is associated with simple, low power, low processing capabilities wireless sensing nodes, it is preferable to use ZigBee to implement the targeted wireless communication.

In ZigBee Network, there are three types of logical devices: the coordinator, the router and the end device, as seen in Figure 13.

- The coordinator: its primary purpose is setting up all the important and major network parameters such as topology, network identification, message propagation, packet size, etc. It is the gateway for the outside world to interact with the network, and it manages all nodes inside the network (Dhillon, Parneet; Sadawarti, Harsh 2014).
- The router: it serves as the intermediate connection between the source and its destination.
- The end-device: end device in ZigBee can be low-power devices possessing limited processing and computing capabilities. They depend on their parents, either a coordinator or a router, to send readings they received from sensors and switches. Each end device can have up to 240 end nodes.

This network supports star, mesh and tree topologies:

- Star topology: the network consists of the coordinator at the center, and surrounding end devices (nodes). Each node is connected directly to the central coordinator. It can only communicate with the coordinator; thus, any data exchange between end devices can only occur through the coordinator.
- Tree topology: the network consists of the coordinator as its root node, several routers and end devices. All the nodes are connected in the form of the tree hence the network name. The end nodes are connected directly to the coordinator and the router as their children nodes. Each end device can communicate with its parent nodes, i.e the coordinator and router, but there is no direct connection between end devices. They can only communicate with each other through their parent nodes (Dhillon, Parneet; Sadawarti, Harsh 2014).

- Mesh topology: similar to tree topology, mesh network also consists of the coordinator, several routers and one or more end devices. The coordinator can send data to any node in the network. If the node is not in range, the message will be sent to a neighboring node which will forward the message to the destination. The network size can be adjusted by adding or removing nodes. The main advantage of this topology compared to the others is its capability of self-healing during the transmission i.e. if any path fails, the node will find an alternative path (Dhillon, Parneet; Sadawarti, Harsh 2014).

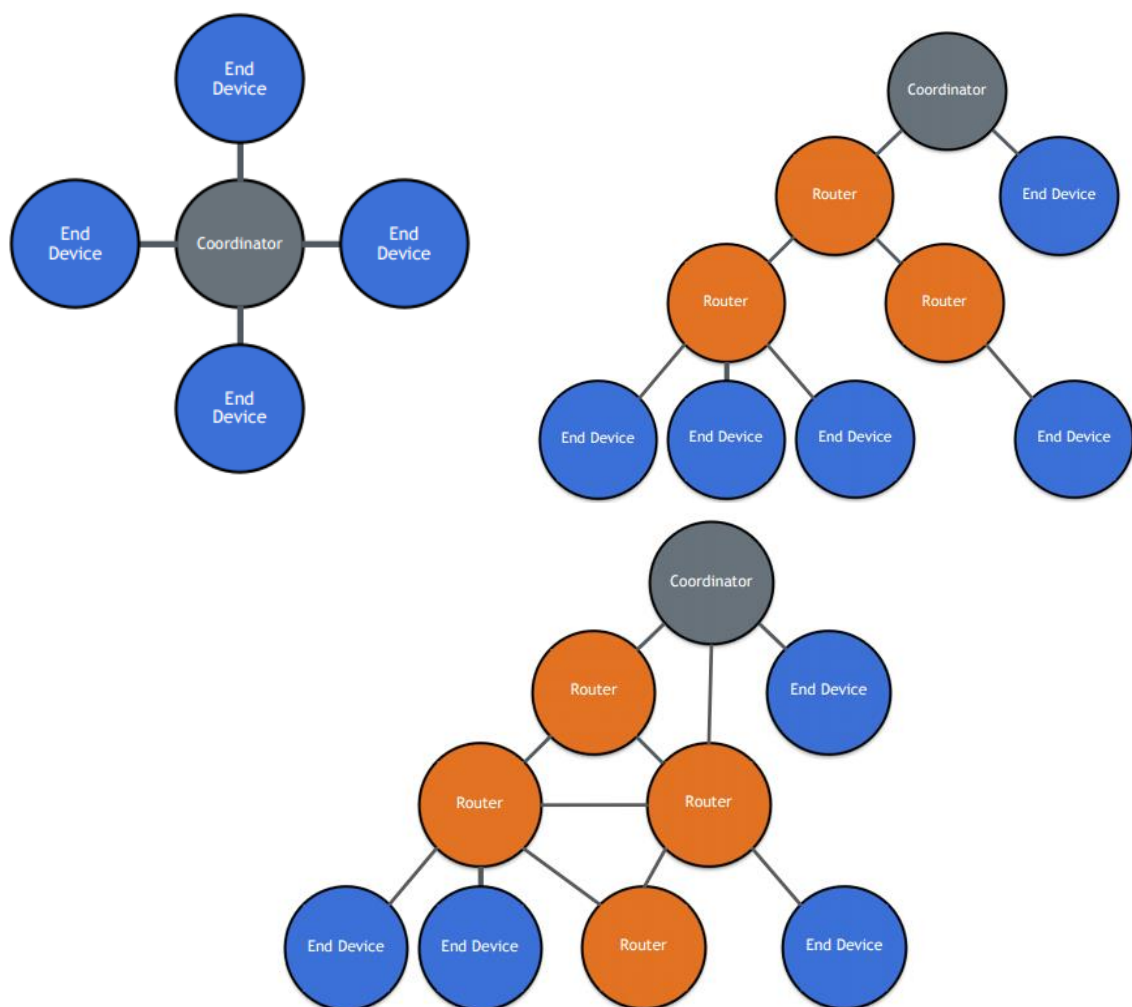


Figure 13: Three supported network topologies of ZigBee (Source: ZigBee Network - MWR Infosecurity).

In a ZigBee Network, individual devices have two address, a MAC address underlined by IEEE 802.15.4 protocol and Network Address, which is a part of ZigBee itself.

- The Media Access Control (MAC Address) is the 64-bit unique identifier, which is normally assigned at the time of manufacture, of the device for network communication. In ZigBee, MAC address is rarely used except when the mapping between MAC address and Network address is needed (Mat Hillman - MWR Info Security).
- The Network Address is the 16-bit address unique identifier assigned to the device within an individual ZigBee Network only. The Coordinator in the network has the address 0x000.

Two identities are used to identify a ZigBee network, the Personal Area Network ID (PAN ID) and the Extended PAN ID (EPID):

- The PAN ID belonged to IEEE 802.15.4 protocol is a 16-bit identifier selected randomly by the Coordinator when the network starts up (Hillman, Matt -MWR Infosecurity).
- The EPID is the 64-bit identifier used to increase the uniqueness of ZigBee's identification, especially when resolving PAN ID conflicts.

For the messages in this network, they can be sent to a specific node, to a group of nodes and to all of the nodes in the entire network. Below is an overview of all these scenarios in ZigBee:

- Unicast: Messages are directed towards a single node in Unicast mode. At the Network level a Network Acknowledgement (ACK), which acts as a feedback to signify whether a receipt of response occurs, will be sent to the original node once the message has reached its destination. At the MAC level, the feedback MAC ACK will be sent between each hop as the message propagates.
- Group Multicast: in this mode, messages are sent simultaneously to a group of nodes. A Network Address configured for group addressing is provided as the destination for the message. In general, Group Multicast is basically Broadcast Mode with an additional event, which is each node checks whether it has Endpoints in the group before processing the message.

- Broadcast: loosely based on the same mechanism included in IEEE 802.15.4, when a broadcast is sent, any Coordinator or Router in range will retransmit it unless the maximum number of retransmission is not reached. A process of passive ACK is used to ensure the reliability without requiring additional message transmission. When a device transmits or retransmits a broadcast, it will hear its surrounding neighbors to ensure they also retransmit the broadcast. If they do not, it will send it again (Hillman, Matt - MWR Infosecurity). Predefined Broadcast Addresses are used to identify broadcast messages. Here is the list of these addresses:  
0xFFFF –Broadcast to all devices  
0xFFFFD –Broadcast to all devices with receiver turn on permanently  
0xFFFFC –Broadcast to all Routers and Coordinators.  
0xFFFB –Broadcast to all low-power Routers.

There are also other methods of message propagation though uncommonly used, and obviously not within the range of this study, in ZigBee such as the Bound Transfer and the Inter-PAN Transfer.



## 5 Development of the System

This chapter is about contents of the system in terms of its functional structure, architecture, and operating principle. Detailed information about the system performance and the integrated performance, together with their respective evaluations, are presented in the following chapter.

### 5.1 Methods and Resources

The development phase consisted of four main phases illustrated in the form of product breakdown structure (PBS) as seen in Figure 14: hardware design, software augmentation, system testing and documenting, in which the first three constitutes up to 90% of the whole period.

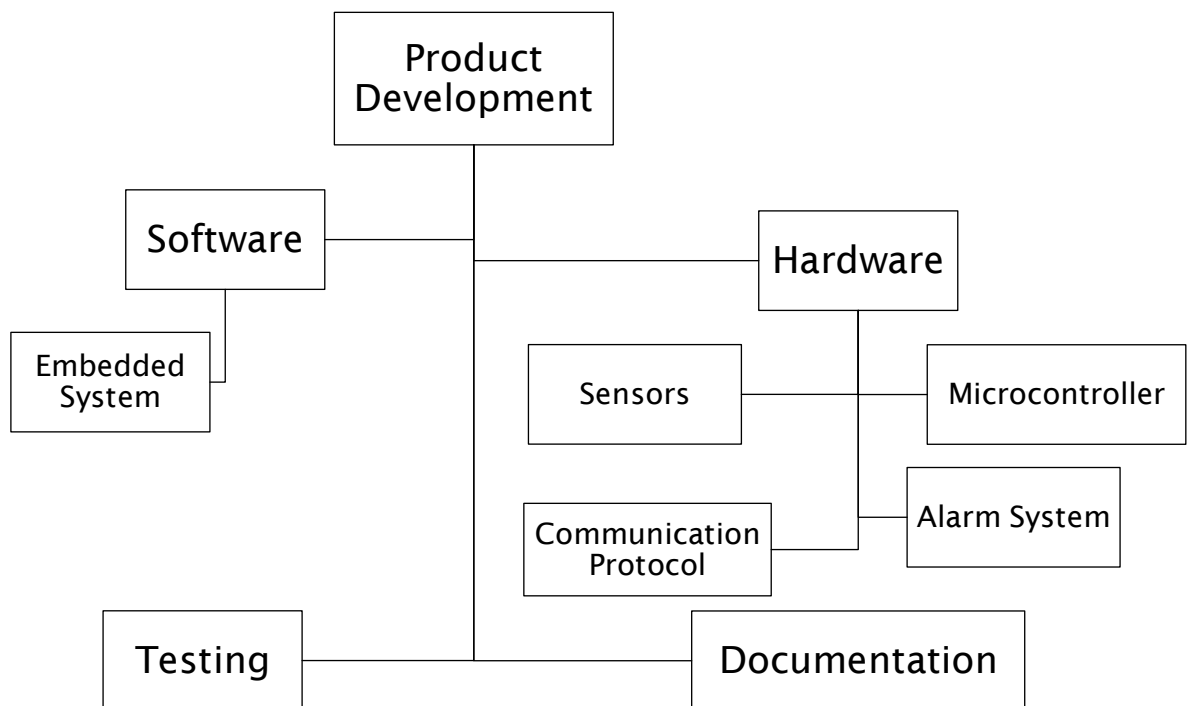


Figure 14: Product Breakdown Structure (PBS) for the Safety System.

For the hardware phase:

- Arduino devices were used as the main microcontrollers because they were easy-to-build, easy-to-integrate, and low-cost. Different versions of

Arduino devices such as Arduino UNO, and Arduino Nano were used during the process.

- Integrated sensors were HC-SR04 ultrasonic sensors, Open PIR motion sensors and Accelerometer. During the ending period, the HC-SR04 sensors were replaced by HRLV-MaxSonar-EZ0s sensor.
- The communication protocol was finalized as the wireless point-to-point using XBee S1 modules. These modules were based on the IEEE 802.15.4-2003 standard designed for point-to-point and star communications at over-the-air baud rates of 250kbit/s, and they possessed these following features: long range, high power transmission, low power consumption, and were P2MP supported in Broadcast Mode (Digikey Website).

For the software phase, the Arduino IDE was used as the main development environment

- The Arduino IDE, which is an abbreviation of Arduino Integrated Development Environment, is a cross-platform and open-source application commonly used to develop Arduino-command software. Arduino IDE included a code editor, a message area, a text console, a toolbar with buttons for common functions, and hierarchic operation menus.

## 5.2 Overview of the System

Through the development phase, two prototypes have been created and tested.

The first prototype consists of these main modules, which is presented in Figure 15: a power supply unit; a distance measurement sensor; a microcontroller; and finally an alarm system.

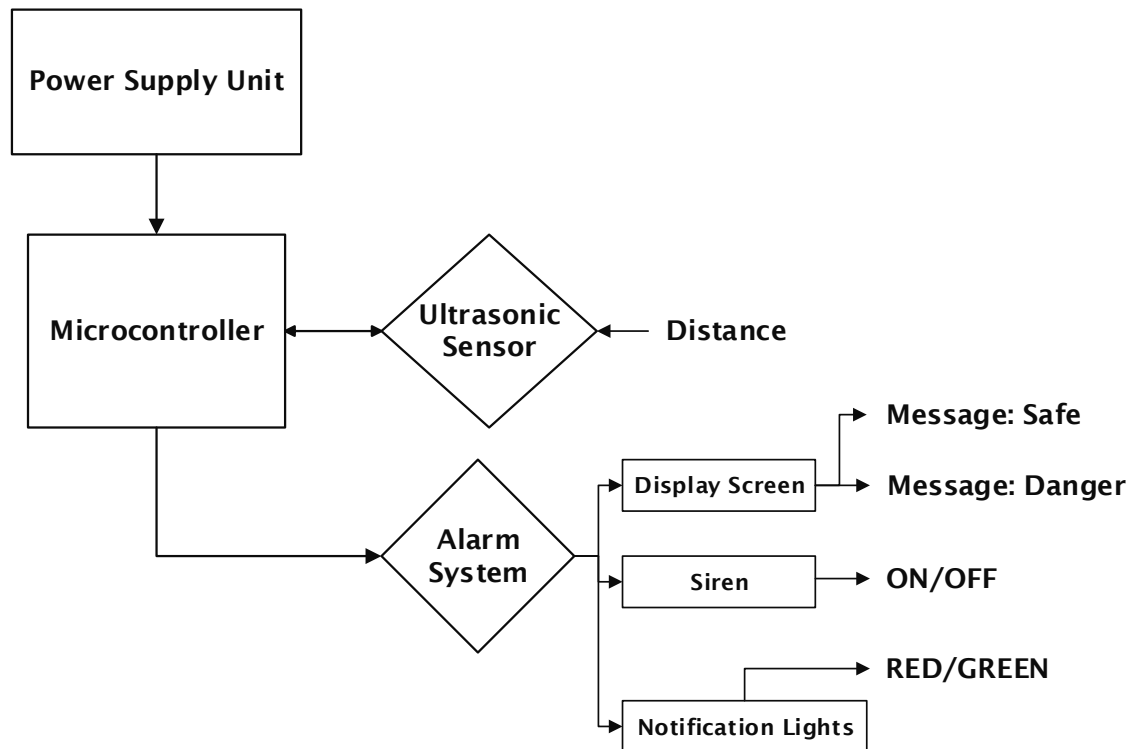


Figure 15: Block diagram of the first prototype.

Below is a summarized explanation about the operating principle of this prototype:

- The ultrasonic sensor detects its surrounding area whether there is a presence of any object within its line-of-sight (L.O.S). If there is an object present, the sensor will determine the distance between the object and it, and send readings to the microcontroller.
- The microcontroller compares the received readings from the sensor with the pre-set safety parameter (the value is set to be two meters). In the case that there is a reading whose value is less than the safety parameter, the Arduino will send a command to commend the alarm system
- The alarm system upon received the command from the microcontroller will turn on the warning notification light (red LED) and the piezoelectric siren configured to ring at 2.6kHz, which is the most sensitive frequency to human ears; concurrently, a message “Someone is within a danger zone” will be displaying on the display screen.
- The alarm system will continue to run until there is no below-the-threshold readings. In that case, the safe notification light (green LED) will

be turned on, and the display screen will display the message “Everything is in order”.

Moving to the second and final prototype, this one has several additional features: it is now equipped with power monitor module, wireless communication modules; two types of sensors (PIR and ultrasonic sensors) to increase the accuracy of human presence detection task.

To sum of, the second prototype now consists of two separate interconnecting entities: a transceiver and a receiver (Figure 16 and Figure 17). Each entity has a power supply unit, which now possesses additional auxiliary modules such as self-regulating power monitor module to provide constant supply voltage for the system and an included fuse to prevent the system from damage caused by excess current; a microcontroller; a communication unit; an alarm system, of which each entity has a different composition.

In this prototype, the transceiver exclusively had the human presence detection.

The operating principle of this prototype is relatively similar to the first prototype:

- After being installed and turned on, the transceiver checks the current power supply status by measuring the supply voltage and current. The module will automatically adjust when it experiences any changes in the supply voltage via a step-up/step-down converter in order to maintain a constant voltage to the system. The receiver conducts the same initial process like in the transceiver.
- Next, the transceiver is assigned to be in power savings mode, and this mode can only be revoked if the PIR sensor notices any human movement within its L.O.S. In the case that such movement is detected, the system will start to conduct the safety check procedure to determine his or her distance. If there is a distance reading below the safety threshold (set to be two meters like in the previous prototype), the transceiver will send a command to commence its integrated alarm system and concurrently send an associated notification to the receiver placed at the worker to turn the receiver’s alarm module on.

- When the situation becomes safe again (no human presence within the below-threshold vicinity), both the transceiver and the receiver turn off their respective alarm modules. Moving to next phase, the transceiver checks its current power level then goes back to the power savings mode.

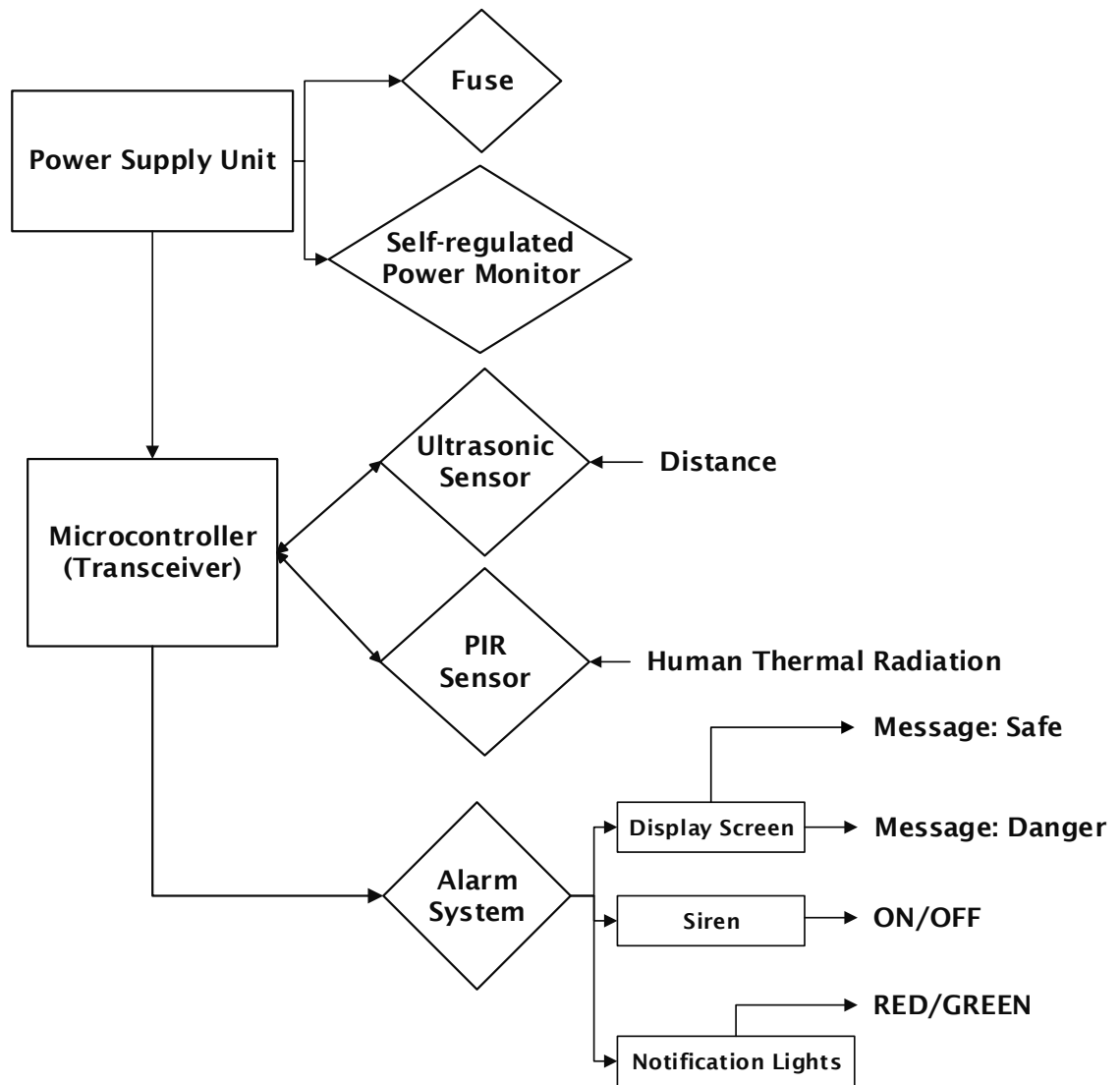


Figure 16: Block diagram of the Transceiver in the second prototype.

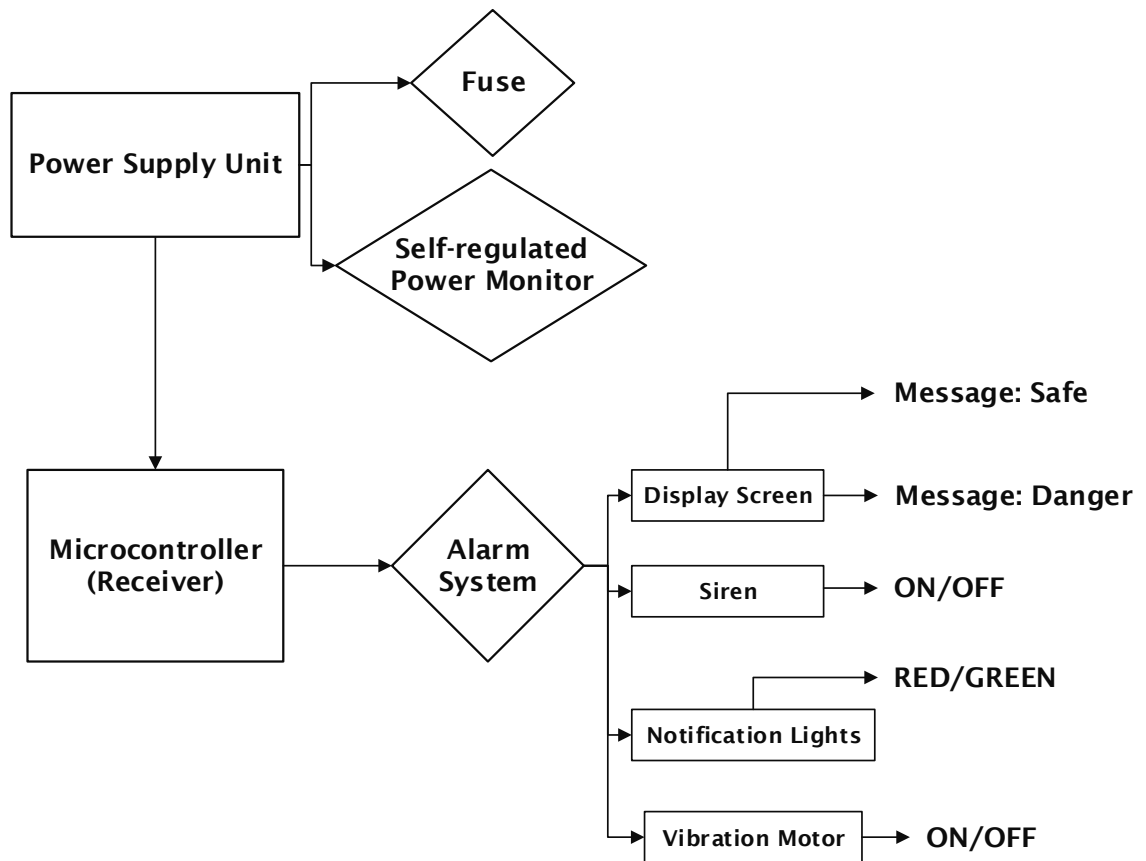


Figure 17: Block diagram of the Receiver in the second prototype.

## 6 Performance Test & Evaluation

This chapter is about the presentation of the system performance results and their evaluation acquired from every module ranging from sensors, microcontrollers, to auxiliary modules in the two developed prototypes mentioned in the last chapter. These results are invaluable as they would contribute to the prospect of perfecting the future final product for industrial manufacturing.

### 6.1 First Prototype Performance Test

#### 6.1.1 Test Procedure

The first prototype was tested in two different environments: the indoor and the outdoor environment. For the outdoor environment, there were two separated test cases: when the system was placed in the defined test site area, and when it was attached and secured to a small excavator placed in the test site area.

The main target test was to determine and evaluate whether the performance of the given ultrasonic sensor – the HC-SR04, was sufficient to be selected as the main distance measurement module. To complete this target, the sensor was subjected to the defined standard layout based on its datasheet, which are presented in Table 4, illustrated in Figure 18:

- The test site surrounding the object-under-test (O.U.T) was cleared of other objects or,
- If the above condition had not been possible to meet, there must be no trivial object within the L.O.S of the sensor.
- The sensor was linked with the siren and was configured so that when the distance readings the sensor acquire was less than  $D_{safety} = 4m$ , the siren would turn on.
- The O.U.T was moved across the sensor with difference speeds to determine its sensitivity and its real measuring angle.

Table 4: Highlight features of the HC-SR04 features.

HC-SR04	
Operating Range	2cm up to 4m
Resolution	1 mm up to 3mm
Operating Frequency	40kHz
Measuring Angle	15 °

$L$  = measurement distance  
(ranging from 1 m up to 4m)

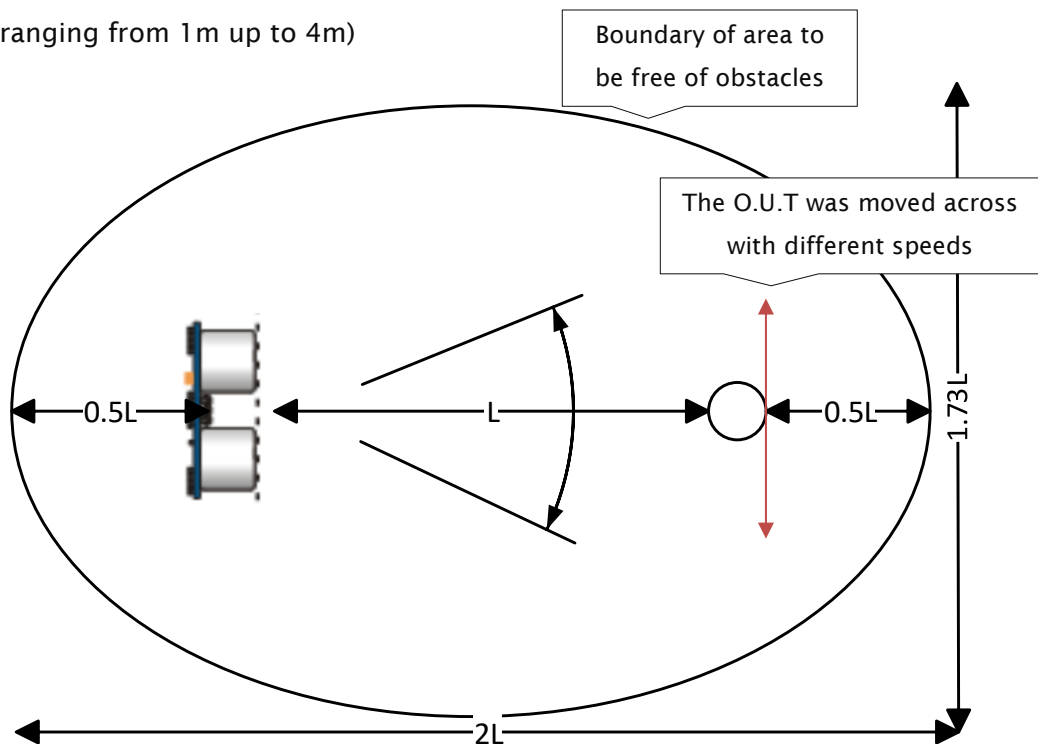


Figure 18: The Test Site Layout for HC-SR04.

#### 6.1.2 Performance Results of the Ultrasonic Sensors

The HC-SR04 ultrasonic sensor was concluded to be relatively unreliable for long-range distance measurement, which are explained below:

Both in the indoor and the outdoor environment test, the readings given by sensors within the equal-or-below three-meter distance were sufficiently reliable. Above three-meter, the accuracy drastically decreased. Thus, the operating range was determined to be based on the possibly acquired readings:



$$D_{operation} = 3 \pm 5\% (m)$$

The furthest distance the sensor was able to measure was 3.3m, which was lower than the predefined safety parameter.

The O.U.T could only be detected if and only if it was not a soft object, its surface was flat or at least had no recognizable curves because it would allow the transmitted ultrasonic waves to be easily reflected upon being incident to the O.U.T, and for the reflected waves to be detectable by the sensing element. If the incident angle between the transmitted waves and the O.U.T was less than  $45^\circ$ , it would not be detected. Besides, the sensor sensitivity proved to be a major issue: when the O.U.T was being moved with the approximate running velocity and acceleration, the HC-SR04 did not generate any readings. These drawbacks are depicted in Figure 19:

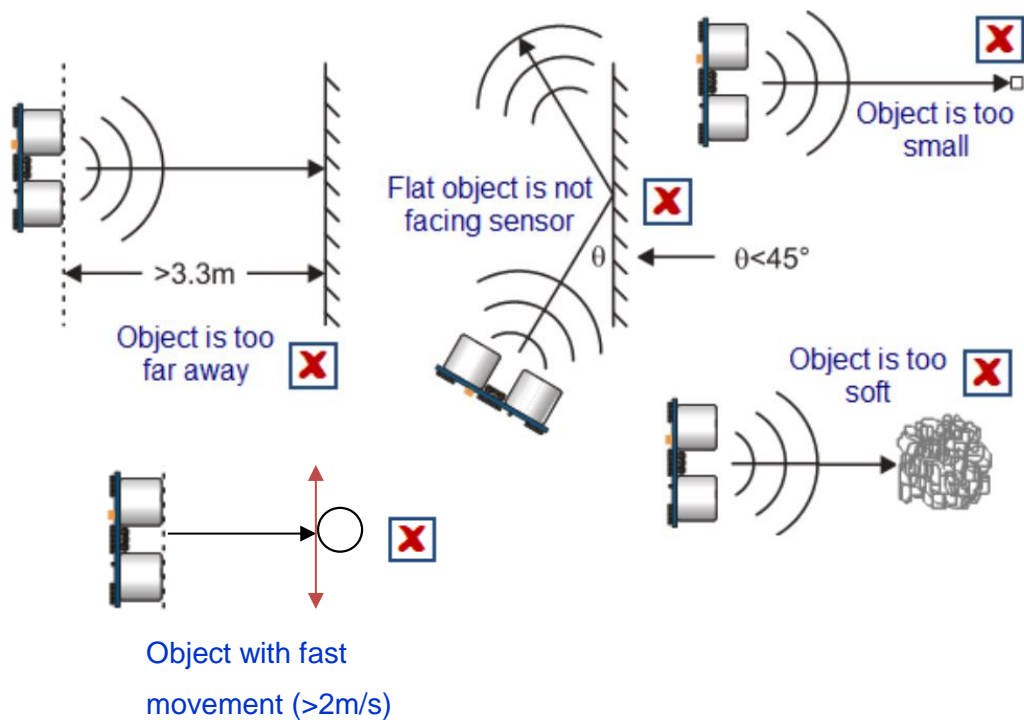


Figure 19: Drawbacks of the HC-SR04 sensor based on its performance test results.

Sufficiently to conclude, the HC-SR04 was the non grata sensor to be included for the system, and a new sensor must be chosen.

Two potential candidates for the new ultrasonic sensor were chosen as the replacement: the HRLV-MaxSonar EZ; and the XL-MaxSonar WR, both of these were available to be purchased immediately through Sparkfun. Their main benefits are listed in Table 5 below:

Table 5: List of the main benefits and drawbacks of the two candidates for new ultrasonic sensor.

	HRLV-MaxSonar EZ1	XL-MaxSonar WR1
Benefits	<ul style="list-style-type: none"> <li>• Low cost ultrasonic range finder.</li> <li>• Reliable and stable range data.</li> <li>• High resolution</li> <li>• Very low power consumption.</li> <li>• Fast measurement cycles</li> </ul>	<ul style="list-style-type: none"> <li>• Acoustic/electrical noise resistance.</li> <li>• Reliable and stable range data.</li> <li>• Robust and low cost IP67 standard.</li> <li>• Narrow beam characteristics.</li> <li>• Very low power consumption</li> </ul>
Drawbacks	<ul style="list-style-type: none"> <li>• Vulnerable to weather.</li> <li>• Average immunity to noises.</li> </ul>	<ul style="list-style-type: none"> <li>• Expensive.</li> </ul>

## 6.2 Second Prototype Performance Test

### 6.2.1 Test Procedure

The second prototype was tested with the same procedure as in the first prototype: tests were conducted in both indoor and outdoor environments. However, there was a minor difference that only one test case –when the system was placed in the define test site without installing to any excavator, was employed when the environment was outdoor and it was not possible to test the accelerometer. These setbacks were due to the unexpected unavailability of an excavator to conduct the test.

The target test goal was relatively wider than the previous ones: the main objectives now were:

- To determine whether the human presence detection module, now with new ultrasonic sensors and PIR sensors, was able to determine any human presence within four-meter perimeter without any significant delay
- The communication between the transceiver and the receiver was successfully established.
- Other modules were able to execute their respective define tasks. Though, the power monitor module was not required to perform its task with high efficiency.

To complete the first objectives, all the sensors were subjected to many tests in their absolute rating configurations layout, and many tests with varying test conditions were conducted. The test site layout, which was based on the features of the sensor mentioned in Table 6, and the test method for the PIR sensor are depicted in Figure 20 and explained below:

- The test site surrounding the person-under-test (O.U.T) was cleared of other thermal-radiated objects,
- The sensor was linked with the siren and was configured so that when the sensor acquired any human presence/movement, the siren would turn on.

- The P.U.T was moved across the sensor's L.O.S with difference speeds to determine the real measuring angle, and the P.U.T would dress with different clothes, especially insulated ones, to determine its sensitivity.
- The sensor would be tested in outdoor environments with varying environment temperatures to determine its influence's weight to the sensor sensitivity.

The test layout and the corresponded test method for the ultrasonic sensor remained the same as in the previous prototype.

$L$  = measurement distance  
(ranging from 1m up to 5m)

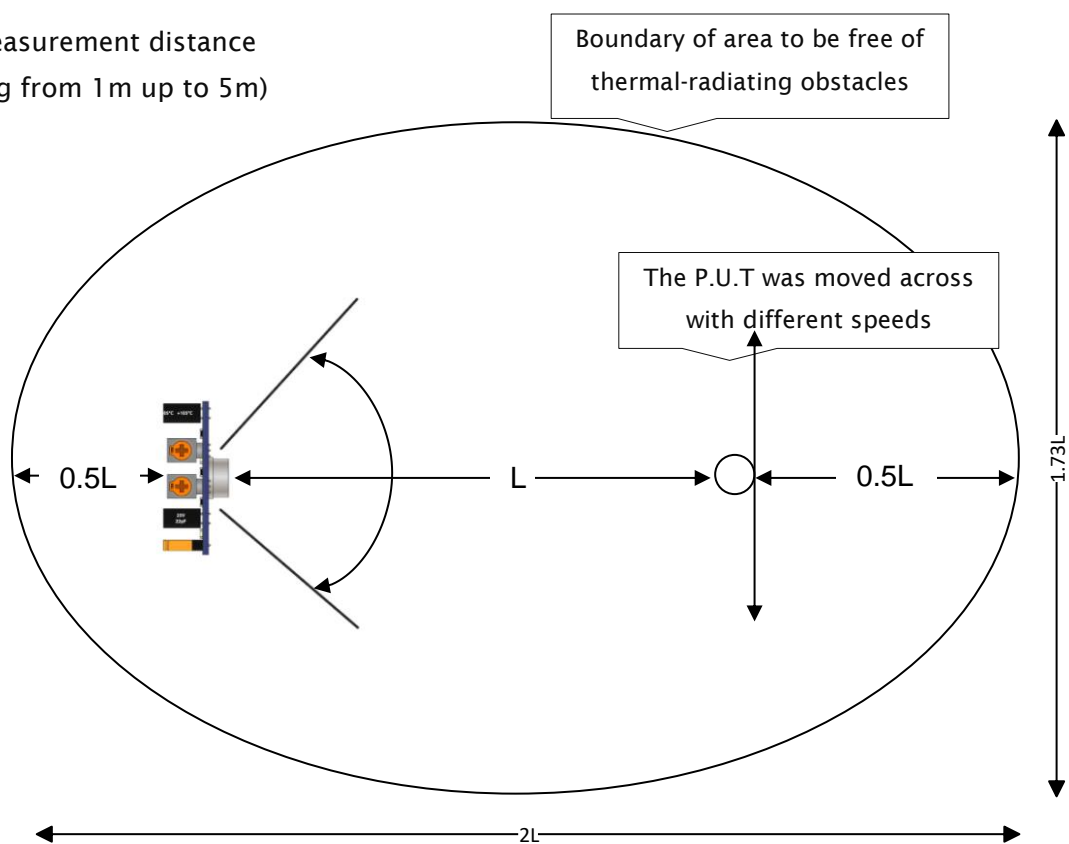


Figure 20: Test Site Layout of the PIR sensor.

Table 6: Highlight features of the Open PIR sensor.

Open PIR (NCS36000)	
Operating Range	1m up to 5m
Operating Temperature	-30 °C up to 80 °C
Measuring Angle	120°

Thanks to the successfully established wireless communication protocol, it was possible to setup an additional item in the above test methods, that when the sensors, which were installed on the Transceiver, the Transceiver would send all the readings to the Receiver connecting to a PC for easy monitoring. This process is described and its subsequent result is illustrated below in Figure 21.

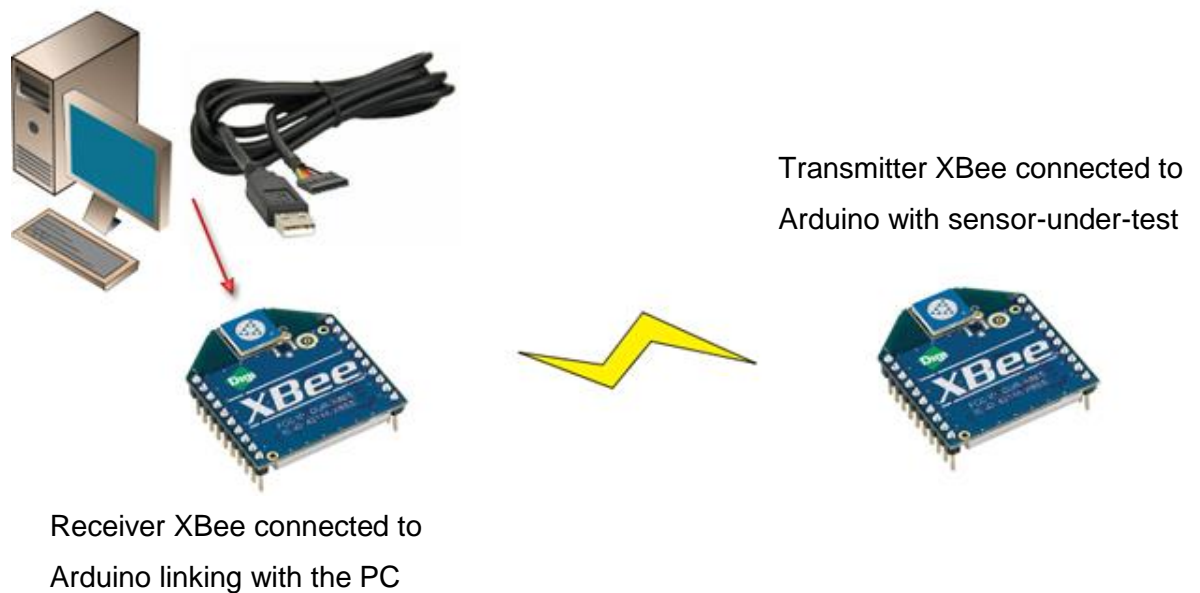


Figure 21: Arduino-to-Arduino Communication Setup for Sensor Performance Test.

### 6.2.2 Performance Test Results of PIR Sensors

The operating performance of the PIR sensors are described in Table 7 below. In indoor environment, the sensor was configured at maximum sensitivity and maximum oscillation frequency, in order to clearly the absolute possible performance rating.

Table 7: Performance results of PIR sensor in indoor environment.

	Test conditions	Results
1	<ul style="list-style-type: none"> <li>Indoor environment with many surrounding obstacles.</li> <li>'Darkroom' lighting condition.</li> </ul>	<ul style="list-style-type: none"> <li>Maximum detecting range: 5m</li> <li>Real detection angle: 60°</li> </ul>
2	<ul style="list-style-type: none"> <li>Indoor environment with many surrounding obstacles.</li> <li>Average lighting condition.</li> </ul>	<ul style="list-style-type: none"> <li>Maximum detecting range: 4.5m</li> <li>Real detection angle: 60°</li> </ul>
3	<ul style="list-style-type: none"> <li>Indoor environment with many surrounding obstacles.</li> <li>Brightest lighting condition.</li> </ul>	<ul style="list-style-type: none"> <li>Maximum detecting range: 4.5m</li> <li>Real detection angle: 60°</li> </ul>

In the indoor environment, regardless of the variation in lighting condition, the sensor is capable of detecting human presence(s) at the four-meter distance, which is the maximum safety perimeter set above. Besides, after repeating the same tests with the person under test (P.U.T) wearing different set of clothes, including insulated clothes which prevents body heat as well as thermal radiation to escape, the sensor is still capable of identifying the P.U.T with a reduced detection range at maximum 3.5 meters, which is lying within the safety perimeter.

The detailed results for the outdoor environment is provided in the Table 8 below. In outdoor environment, the sensor was also configured at maximum

sensitivity and maximum oscillation frequency with the same intention to clearly the absolute possible performance rating.

Table 8: Performance Results of the Open PIR sensor in the outdoor environment.

	Test conditions	Results
1	<ul style="list-style-type: none"> <li>Outdoor environment with limited surrounding obstacles.</li> <li>Clear and bright weather.</li> </ul>	<ul style="list-style-type: none"> <li>Maximum detecting range: 3.5~4.0m</li> <li>Real detection angle: 120°</li> </ul>
2	<ul style="list-style-type: none"> <li>Outdoor environment with limited surrounding obstacles.</li> <li>Cloudy weather.</li> </ul>	<ul style="list-style-type: none"> <li>Maximum detecting range: 4.0m</li> <li>Real detection angle: 120°</li> </ul>
3	<ul style="list-style-type: none"> <li>Outdoor environment with limited surrounding obstacles.</li> <li>Showering.</li> </ul>	<ul style="list-style-type: none"> <li>Maximum detecting range: 4.0m</li> <li>Real detection angle: 60°</li> </ul>
	<ul style="list-style-type: none"> <li>Outdoor environment with many surrounding obstacles.</li> <li>Clear and bright weather.</li> </ul>	<ul style="list-style-type: none"> <li>Maximum detecting range: 3.5~4.0m.</li> <li>Real detection angle: 80~90°.</li> </ul>

Moving to the outdoor environment, regardless of the variation in weather and temperature (though the fluctuation of the latter is within 3-5°C due to the current season), the sensor is still capable of conducting its intended use. Similarly, in the separate testing with the P.U.T wearing different set of clothes, the retained its performance with only a slight reduced detection range at maximum 3.25m to 3.5m.

Despite its promising performance, the sensor yet suffered several limitations. First, it has a reduced observable angle (60°) compared to the theoretical one (120°) provided in the datasheet, in which the obstacles-filled environment likely act as a main reason for reduced performance. The last and most important of all, the sensor can perceive whether there is a human presence if and only if the P.U.T is moving horizontally across its L.O.S as shown in Figure 23. In a situation

that the P.U.T is moving vertically, in other words, towards or away from the sensor, the PIR can only detect at an immensely close distance, from one to two meters at max, which is a considerable problem based on the nature of work in construction sites requiring a great range of variation in worker's movement.

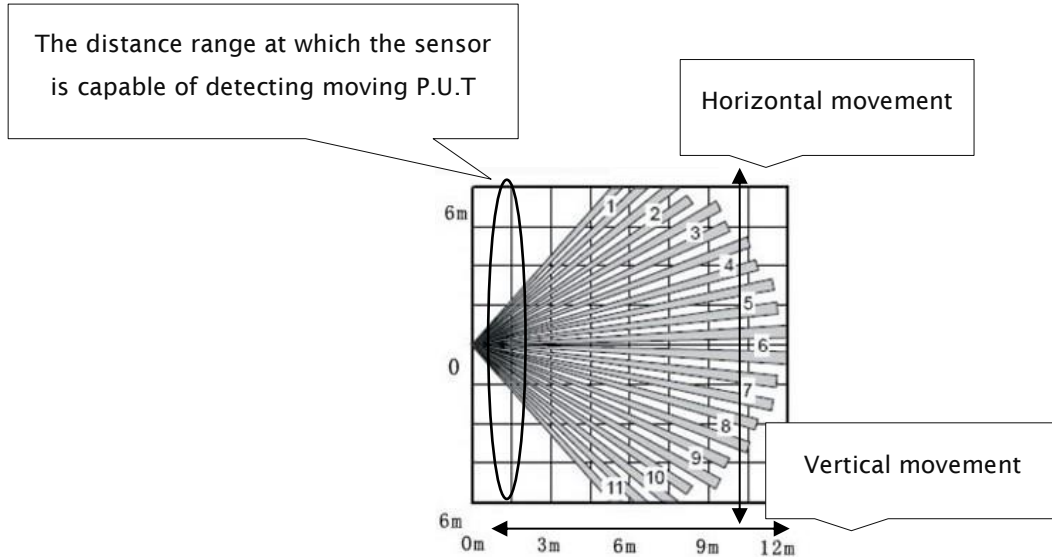


Figure 22: Performance Limitation of Open PIR Sensor.

To sum up, the Open PIR sensor had a relatively great performance based on the above results, despite having several drawbacks. Nevertheless, the author believed that it is possible to furtherly increase its performance by replacing the current Fresnel fabricated from plastics materials with glass-based ones. The lens made from glass material has the higher converging ratio than its plastic counterparts, which would increase the amount of receiving thermal radiations to the sensor, hence the better performance.

### 6.2.3 Performance Test Results of the Power Monitor Module

As mentioned above, the power supply unit consisted of a power monitor based on the application of self-regulated DC-DC voltage converter and a protecting fuse. For self-regulated DC-DC converter, Buck-Boost converter topology was used, and it was implemented by the introduction of the MC34063 micro DC-DC converter. The micro-converter is preferred for this power module design because it offers many advantages, such as great size reduction, and greater



power conversion efficiency compared to conventional designs, which mainly use passive components and semiconductor devices. Table 9 provides a great detail about the comparison between the micro DC-DC design with the conventional one, and the example converter schematic is presented in Figure 23 below.

Table 9: Comparison between the conventional Buck-Boost and the micro DC-DC Buck-Boost Converter.

Conventional Buck-Boost Converter	Micro DC-DC Converter
<ul style="list-style-type: none"> <li>• Pulsed input current, requires input filter.</li> <li>• Pulsed output current increases output voltage ripple</li> <li>• Output voltage can be either greater or smaller than input voltage.</li> </ul>	<ul style="list-style-type: none"> <li>• Continuous input current.</li> <li>• Continuous output current.</li> <li>• Output voltage can be either greater or less than input voltage.</li> <li>• Great size reduction</li> </ul>

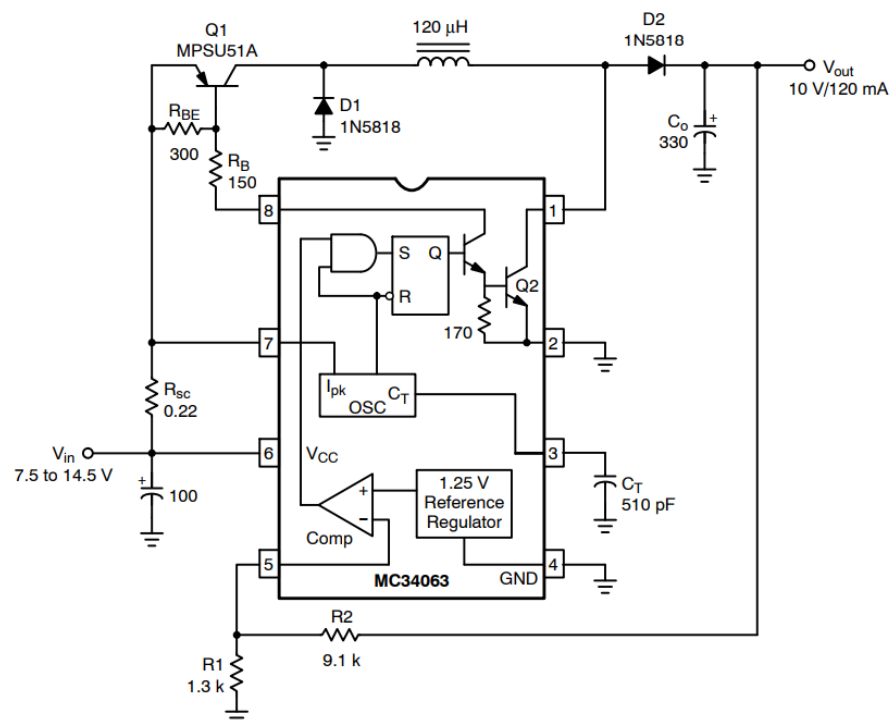


Figure 23: The schematic of the power monitor module (Source: Theory and Applications of the MC34063 Switching Regulator Control Circuits – On Semiconductor).

The values for the components of the power monitor modules are computed based on the required design parameters such that:

- The input source voltage varies from 7.5V to 20V.
- The output voltage is 10V.
- The switching frequency is 50kHz.
- The maximum output current is 120mA.
- The maximum ripple voltage is 1% of the output voltage or 100mVp-p.

The following design procedure, which is based on the design tutorial of MC34063 application design from On Semiconductor, is provided to depict how proper component values for this application were selected.

The ratio of switch condition  $t_{on}$  versus diode conduction time  $t_{off}$  was determined by:

$$\frac{t_{on}}{t_{off}} = \frac{V_{out} + V_{FD1} + V_{FD2}}{V_{in(min)} - V_{satQ1} - V_{satQ2}} = \frac{10 + 0.6 + 0.6}{7.5 - 0.8 - 0.8} = 1.9 \quad (4)$$

The cycle time of LC network is equal to  $t_{on(max)} + t_{off}$ :

$$t_{on(max)} + t_{off} = \frac{1}{f_{min}} = \frac{1}{50 \times 10^3} = 20\mu s \text{ per cycle} \quad (5)$$

The  $t_{on}$  and  $t_{off}$  were calculated from (3) and (4):

$$t_{off} = \frac{t_{on(max)} + t_{off}}{\frac{t_{on}}{t_{off}} + 1} = \frac{20 \times 10^{-6}}{1.9 + 1} = 6.9\mu s \quad (6)$$

$$t_{on} = 20\mu s - 6.9\mu s = 13.1\mu s \quad (7)$$

The maximum on-time was set by selecting a value for  $C_T$ :

$$C_T = 4.0 \times 10^{-5} \times t_{on(max)} = 4.0 \times 10^{-5} \times 13.1 \times 10^{-6} = 524pF \quad (8)$$

The peak switch current is:

$$I_{pk(switch)} = 2 \times I_{out} \times \left( \frac{t_{on}}{t_{out}} + 1 \right) = 2(120 \times 10^{-3})(1.9 + 1) = 696mA \quad (9)$$

A minimum value of inductance was determined by the maximum on-time and peak switch current:

$$L_{min} = \frac{V_{in(min)} - V_{satQ1} - V_{satQ2}}{I_{pk(switch)}} t_{on} = \frac{7.5 - 0.8 - 0.8}{696 \times 10^{-3}} (13.1 \times 10^{-6}) = 111\mu H \quad (10)$$

The current limit resistor  $R_{sc}$  was determined by the current limit level of  $I_{pk(switch)}$  when  $V_{in} = 20V$ :

$$I'_{pk(switch)} = \frac{V_{in} - V_{satQ1} - V_{satQ2}}{L_{min}} t_{on(max)} = \frac{20 - 0.8 - 0.8}{111 \times 10^{-6}} (13.1 \times 10^{-6}) = 2.17A$$

$$R_{sc} = \frac{0.33}{I'_{pk(switch)}} = \frac{0.33}{2.17} = 0.15\Omega \quad (11)$$

The minimum value of output filter capacitor was determined as:

$$C_o = \left( \frac{I_{out}}{V_{ripple(p-p)}} \right) t_{on} = \frac{120 \times 10^{-3}}{100 \times 10^{-3}} (13.1 \times 10^{-6}) = 15.7\mu F \quad (12)$$

The nominal output voltage was programmed by  $R_1$  and  $R_2$  resistor divider:

$$R_2 = R_1 \left( \frac{V_{out}}{V_{ref}} - 1 \right) = R_1 \left( \frac{10}{1.25} - 1 \right) = 7R_1 \quad (13)$$

The base-emitter turn-off resistor  $R_{BE}$  and the base drive resistor  $R_B$  for Q1 were selected to be  $R_{BE} = 287\Omega$  and  $R_B = 151\Omega$ .

The realization of the power monitor module is presented in Figure 24 (in schematic format) and Figure 25 (in layout format) below, of which the latter was used for PCB manufacturing.

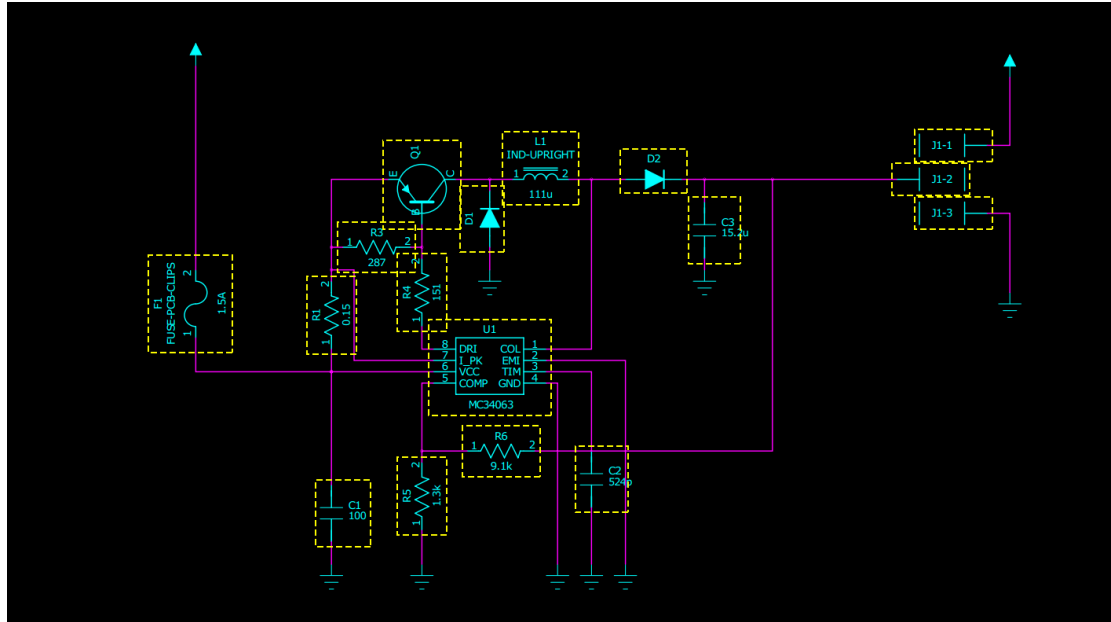


Figure 24: Realization of the power module in schematic format.

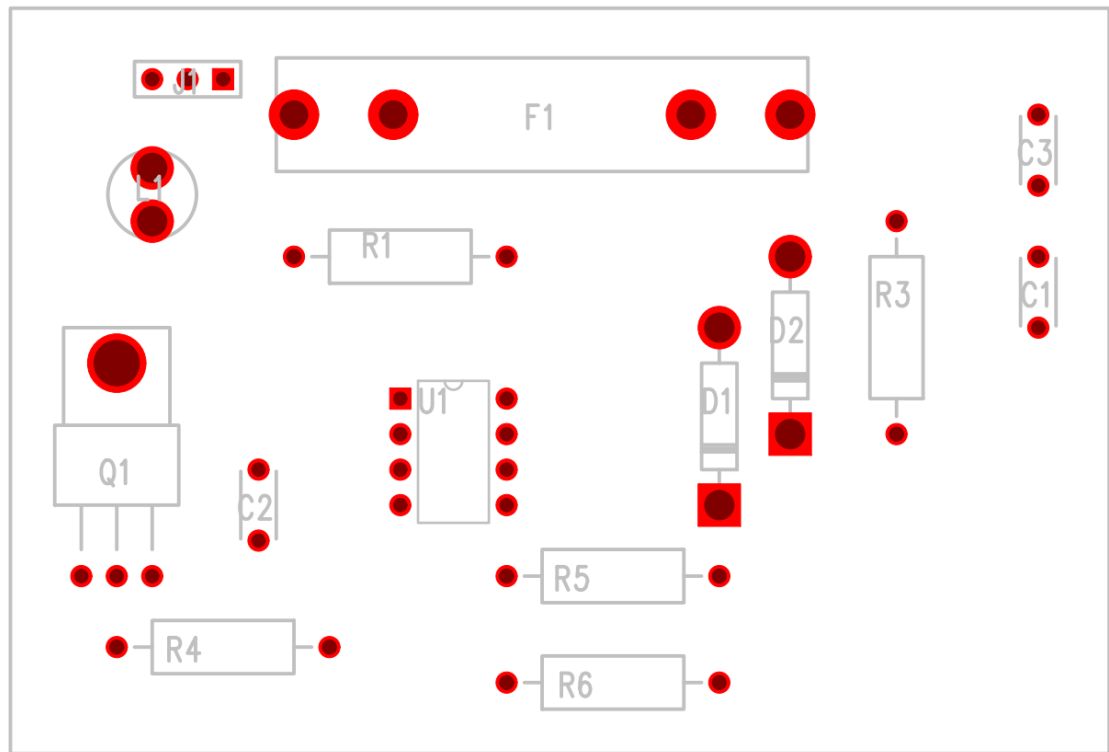
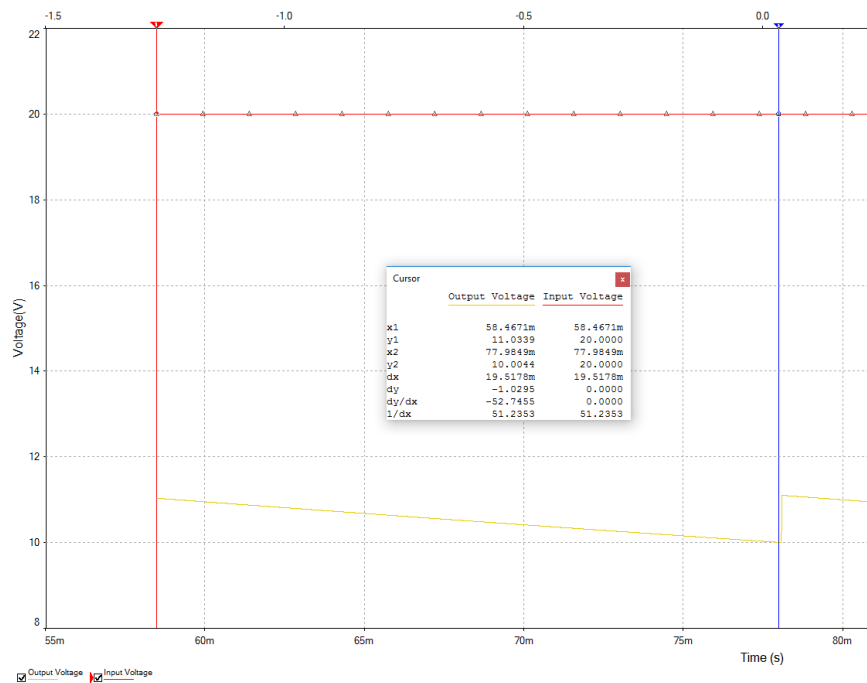


Figure 25: Realization of the power module in layout format for PCB manufacturing,

Figure 26 presents the measurement results of the performance of the power monitor module:



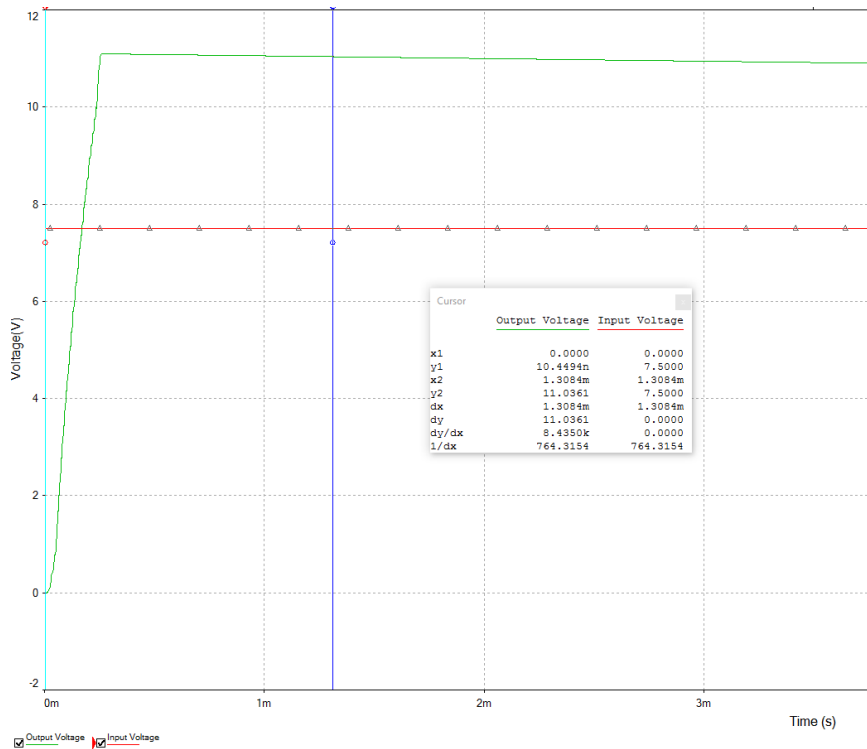


Figure 26: Performance measurement results of the power monitor module.

It is clearly from Figure 26 that the output voltage from power monitor module, which also supplied the microcontroller, was approximately constant voltage at 10V with a noticeable ripple at 20V input voltage when the input voltage was varying from 7.5V to 20V. Therefore, the power monitor was concluded to be working as expected.

#### 6.2.4 Performance Test Results of the new Ultrasonic Sensors

After conducting all the required tests in both indoor and outdoor environments, the author acquired these following results for the HRLV-EZ0 sensor, which are also illustrated in Figure 27:

- The sensor possessed a relatively wide and symmetrical beam width. The maximum measuring angle managed to achieved was  $60^\circ$ .
- The sensor displayed the distance of the nearest object within its L.O.S.

- The sensor was capable of detecting and measuring objects whose speeds could be up to 10m/s.

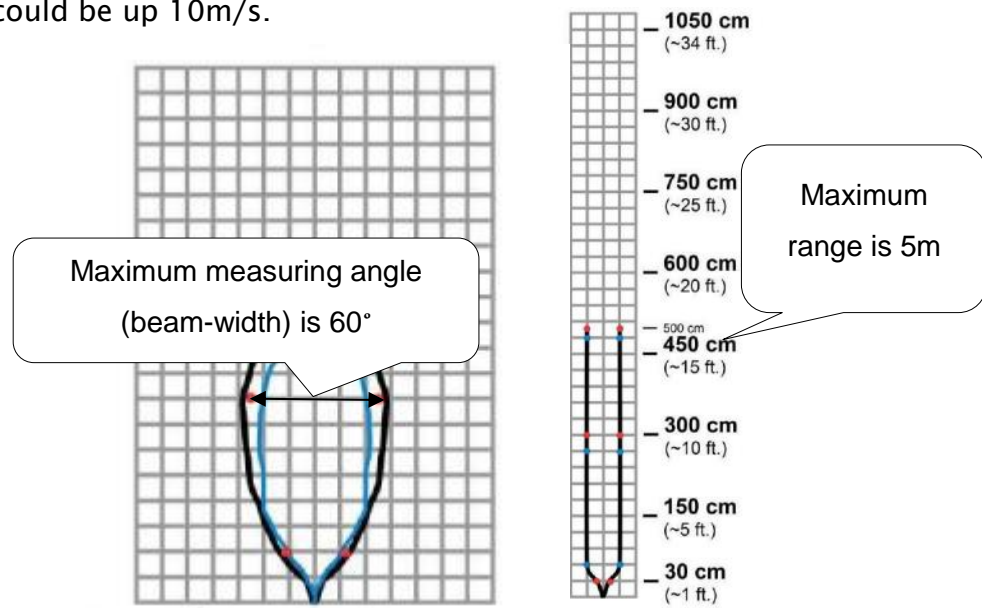


Figure 27: Measurement results of the HRLV-EZ0's performance.

Most important, the author noticed that the actual supply voltage measured at the V+ pin and generated from the microcontroller to the sensor was 4.7V, which influenced the accuracy of the reading. This issue was illustrated in Figure 28 below.

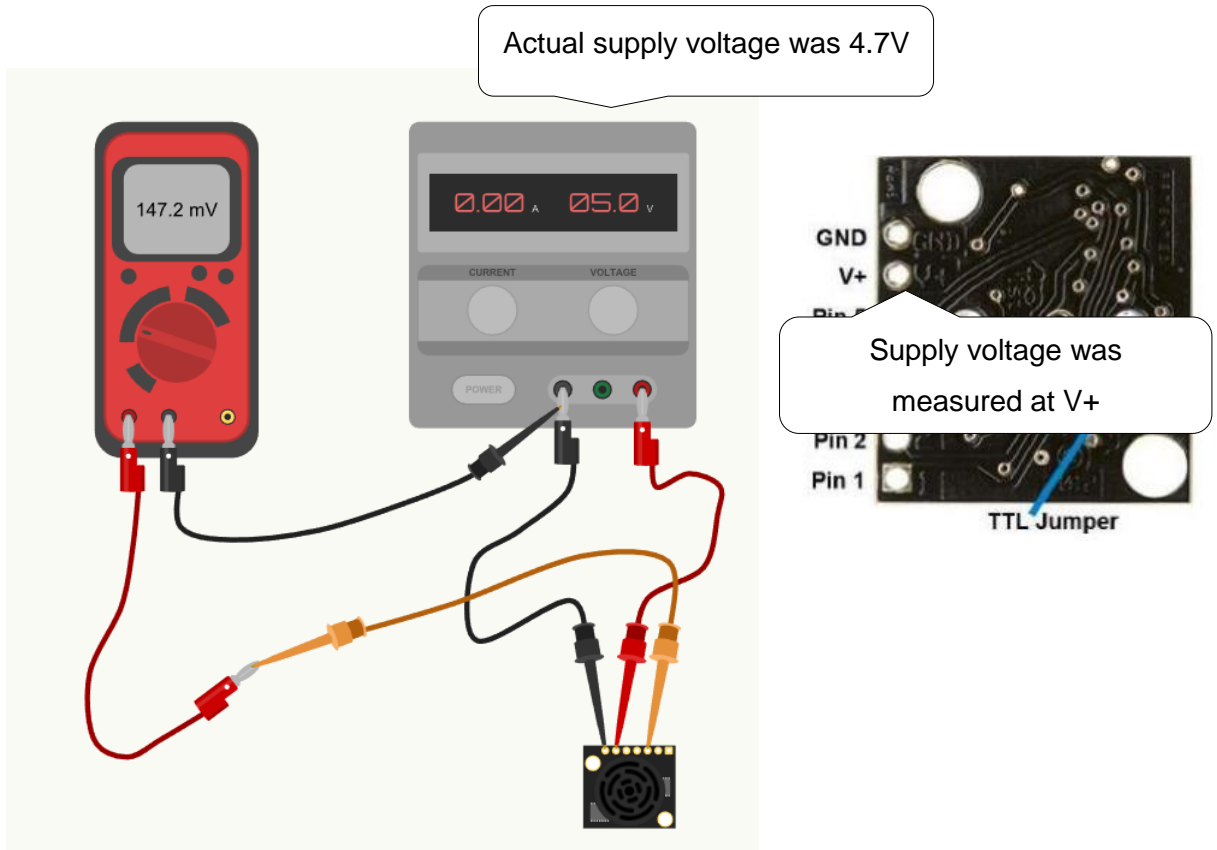


Figure 28: Different supply voltage value than the recommended one in HRLV-EZ0 leads to inaccurate distance measurement.

Assumed the supply voltage is the recommended value, meaning the measured distance when the analog output was measured as 147.2mV is:

$$D_{distance} = 5 \frac{V_m}{V_i} = 5 \frac{(147.2m)}{\frac{5}{1024}} = 177.2288mm \text{ (14)}$$

In which:  $V_m$  is measured voltage at the AN pin of the sensor;

$$V_i \text{ is scaling voltage and } V_i = \frac{V_{cc}}{1024} = \frac{5}{1024} = 0.004883V \text{ per } 5 \text{ mm (15)}$$

The real measured distance with the 4.7V supply voltage is

$$D_{distance} = 5 \frac{V_m}{V_i} = 5 \frac{(147.2m)}{\frac{4.7}{1024}} = 150.7328mm \text{ (16)}$$

The percentage of error is 14.95%, which is noticeable high. As a result, it is recommended that a continuous voltage measurement is implemented to yield accurate distance measurement. Such a voltage measurement can be achieved by the implementation of a comparator device using the microcontroller with its own fixed reference voltage.

However, despite having its own analog inputs capable of accurately measure voltage, and the successive approximation type Analog to Digital converter (ADC) to convert the acquired analog values and its own voltage reference, the reference voltage in the Arduino microcontroller was not sufficiently precise for conducting any accurate measurement. According to the datasheet, the ATmega chip in the Arduino board provides these following reference voltages:

- DEFAULT: the default analog reference of 5V (on 5V-powered Arduino boards) or 3.3V (on 3.3V-powered Arduino boards).
- INTERNAL: a built-in reference, equal to 1.1V on the ATmega168 or ATmega328 and 2.56V on the ATmega8.
- INTERNAL1V1 and INTERNAL2V56: a built-in 1.1V and 2.56V reference voltages respectively only available for Arduino Mega.
- EXTERNAL: the voltage applied to the AREF pin (0 to 5V only).

Nevertheless, the accuracy of these reference voltages from the microcontroller is limited, which was verified by these measurements:

- The DEFAULT voltage value greatly depends on the power supply from the computer. The exact value measured from the USB port is 4.4V to 5.25V.
- As for the INTERNAL1V1 and INTERNAL2V56, the exact measured values are approximately 1.00V to 1.20V and 2.40V to 2.80V respectively.

The accuracy of the reference against whichever voltage is measured - using any of the above references - is at best only 5% of the accuracy class- much worse than the 0.25% of the accuracy class the ADC provide, which is the result from the maximum error ( $\pm 2$  LSB meaning the maximum error is 2 bits-4 decimals, out of 10 bits-1023 decimals, according to the Arduino specification). It is clearly that an alternative approach must be consider to improve the measurement accuracy. Therefore, the author proposed one solution: employing an external shunt voltage reference –in this case, it is the LM4040 precision micro-power shunt voltage reference (Figure 29):



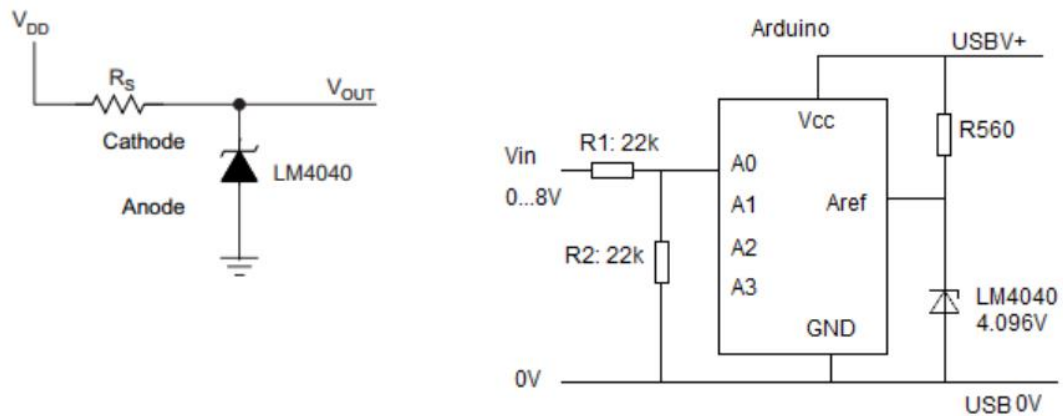


Figure 29: The shunt reference application circuit (left), and the general setup of the application to the Arduino microcontroller (right).

For the conclusion, it is sufficing to say that with the availability of the new ultrasonic sensor -the HRLV-MaxSonar EZ0 (MB1003), the problem about the unreliable distance detection was solved if and only if the supply voltage to the sensor was maintained at the recommended value. In the case such situation was not possible, continuous voltage measurement must be implemented in order to scale the acquired readings to the accurate distance.

## 7 Conclusions and Discussions

To sum up, the goal of this study is to design a safety system, which is able to accurately detect human presence, acting as a solution for accidents caused by excavators. Through the length of this study, it was possible to achieve the target system specification -the active detection of human presence and measuring the distance to warn whether the distance is lower than the safety perimeter with great accuracy, by successfully selecting appropriate components.

However, there are still several main problems listed below, mainly about the instalment of the system to the excavator, and the detection of workers whose tasks require them to be within the danger perimeter (0.5-1 m, according to HSE):

- Thermal Management: the sensor nodes are placed at the blind spots of the excavators, which also have high temperature (up to 60 °C) during the machine operation. As a result, careful thermal management is required to reduce the risk of the system to be malfunction.
- Weather resistance: as the system is used in construction sites; therefore, waterproof, dust proof, pressure and shatter resistant are the must-have included features. Currently, one weather resistance case has been purchased and is waiting for test.
- Exceptional cases: as mentioned above, another method is needed to be figured out for workers working closed to the excavator. One solution is the employment of a separate microcontroller configured only for this case.

As for the conclusion, the designed safety system met the required safety feature. Yet further improvements are necessary to be conducted in the upcoming time in order to completely develop and release the product to the market.

## References

- 1) Fraden, J. (2004). Handbook of Modern Sensors. Springer International Publishing.
- 2) Abrar, Aneela; Cochran, Sandy (2007). Mathematical Optimization of Multilayer Piezoelectric Devices with Non-uniform Layers by Simulated Annealing. IEEE
- 3) Halliday, D. (2014). Fundamentals of Physics. John Wiley.
- 4) Parneet Dhillon; Harsh Sadawarti (2014). Impact Analysis on the Performance of ZigBee Protocol Under Various Mobility Models. International Journal of Engineering Trends and Technology (IJETT).
- 5) Hillman, Matt. An Overview of ZigBee Networks. MWR InfoSecurity.
- 6) HSE UK Government. (2017). Construction - Excavator industry health & safety. Available at:  
<http://www.hse.gov.uk/construction/safetytopics/excavators.htm>  
 [Accessed 20 Sep. 2017].
- 7) Worksafe New Zealand. Excavation Safety – Worksafe Construction. Available at: <http://construction.worksafe.govt.nz/guides/excavation-safety> [Accessed 18 Oct. 2017].
- 8) Lifewire. (2017). What Is the OSI Model?  
 Available at: <https://www.lifewire.com/open-systems-interconnection-model-816290> [Accessed 18 Jun. 2017].
- 9) Duncan Haughey. (2015) 'Project Management Tools', Project Smart. Available at: <https://www.projectsmart.co.uk/project-management-tools.php> [Accessed 30 June. 2017].

- 10) Digi Key. XBee Low-power module with PCB antenna. Available at: <https://www.digi.com/products/models/xb24-api-001> [Accessed 18 Oct. 2017].
- 11) On Semiconductor (2013). Theory and Applications of the MC34063 and  $\mu$ A78S40 Switching Regulator Control Circuits. Semiconductor Components Industries, LLC.

## Appendix

## Appendix A

The list of the accident cases, together with their associated studies caused by excavator operation in industries, provided by the Worker's Compensation Centre in Finland.

Tunnus	Otsikko		
TOT 1/16	Työntekijä jäi maansortuman alle rivitalon viemäritöissä	[Tarkemmat tiedot]	[Raportti pdf-muodossa]
TOT 5/11	Työkoneen seisonajarrun käyttämättömyyteen liittyvät työpaikkakuolemantapaukset (teematutkinta)	[Tarkemmat tiedot]	[Raportti pdf-muodossa]
TOT 1/11	Rusnattava kivi putosi louhintatyöntekijän päälle	[Tarkemmat tiedot]	[Raportti pdf-muodossa]
YTOT 3/10	Viemäryömaalla työskennellyt aliurakoitsija jäi kaivinkoneen yliajamaksi	[Tarkemmat tiedot]	[Raportti pdf-muodossa]
YTOT 1/10	Yrittäjä hukkui kuljettamansa kaivukoneen pudottua jäiden läpi	[Tarkemmat tiedot]	[Raportti pdf-muodossa]
TOT 10/09	Panostajan apulainen putosi louhokseen kompressorin työntämänä	[Tarkemmat tiedot]	[Raportti pdf-muodossa]
TOT 5/09	Kaivinkoneen kuljettaja hukkui kaivinkoneen pudottua proomusta	[Tarkemmat tiedot]	[Raportti pdf-muodossa]
TOT 17/08	Toimitusjohtaja jäi sorakuopalla pyöräkuormaajan alle	[Tarkemmat tiedot]	[Raportti pdf-muodossa]
TOT 24/07	Panostaja jäi peruuttavan kuorma-auton alle	[Tarkemmat tiedot]	[Raportti pdf-muodossa]
TOT 3/07	Työkoneenkuljettaja hukkui puskutraktorin suistuttua mereen	[Tarkemmat tiedot]	[Raportti pdf-muodossa]
TOT 21/06	Kaivinkoneenkuljettaja kuoli kallioräjäytyksessä	[Tarkemmat tiedot]	[Raportti pdf-muodossa]
TOT 24/05	Traktorin kuljettaja jäi takapyörän ja turvejyrsimen yliajamaksi	[Tarkemmat tiedot]	[Raportti pdf-muodossa]
TOT 20/05	Kuljettaja jäi kaivinkoneen alle	[Tarkemmat tiedot]	[Raportti pdf-muodossa]
TOT 16/03	Aliurakoitsijan työntekijä menehtyi ajettuaan puskutraktorin niin lähelle avolouhoksen rintausta, että puskutraktori putosi alas 15 metrin matkan	[Tarkemmat tiedot]	[Raportti pdf-muodossa]
TOT 8/03	Työkoneenkuljettaja hukkui, kun kaivukone upposi jäihin vesijohtotyömaalla	[Tarkemmat tiedot]	[Raportti pdf-muodossa]

TOT 4/03	Kaksi kaivukoneenkuljettajaa jäi sora- ja kiviaineksen alle, kun sorakuopan reuna sortui äkillisesti	[Tarkemmat tiedot]	[Raportti pdf-muodossa]
TOT 6/02	Autonkuljettaja jäi perävaunullisen kuorma-auton ja pyöräkuormaajan väliin	[Tarkemmat tiedot]	[Raportti pdf-muodossa]
TOT 3/02	Kivityöntekijä jäi kalliosta irronneen lohkareen alle	[Tarkemmat tiedot]	[Raportti pdf-muodossa]
TOT 6/99	Maansiirtoauto vyöryi takaperin jyrkänteeltä alas 50 metrin matkan, kuljettaja lensi ohjaamosta jäädessä auton alle	[Tarkemmat tiedot]	[Raportti pdf-muodossa]
TOT 13/98	Purettavan muuntajan vesikatto sortui, päällä työskennellyt jäi alle	[Tarkemmat tiedot]	[Raportti pdf-muodossa]
TOT 3/98	Kaivannon seinämä murtui kaivinkoneenkuljettajan päälle	[Tarkemmat tiedot]	[Raportti pdf-muodossa]
TOT 36/97	Kuorma-autonkuljettaja jäi kaivinkoneen työkalukaapin oven ja siirtolavan väliin leikkaavaan puristukseen	[Tarkemmat tiedot]	[Raportti pdf-muodossa]
TOT 25/96	Kaatuva sähköpylväs iski asentajaa päähän	[Tarkemmat tiedot]	[Raportti pdf-muodossa]
TOT 23/96	Poraaja oli pulittaamassa ajoneuvolla tunnelin perään, kun noin 10 tn irtokiveä sortui päälle	[Tarkemmat tiedot]	[Raportti pdf-muodossa]
TOT 2/96	Kaivinkoneenkuljettaja hukkui jään pettäessä ja telakaivurin kaaduttua lampeen	[Tarkemmat tiedot]	[Raportti pdf-muodossa]
TOT 1/96	Työnjohtaja puristui kuoliaaksi kaivinkoneen ylävaunun ja kallion välissä	[Tarkemmat tiedot]	[Raportti pdf-muodossa]
TOT 4/95	Sorakuopan lipan alla kaivinkonetta korjaamassa ollut kaivinkoneenkuljettaja jäi jäätyneen sorakimpaleen alle	[Tarkemmat tiedot]	[Raportti pdf-muodossa]
TOT 3/95	Maanrakennustyömaalla kaivinkone suistui jään peittämään rantaveteen	[Tarkemmat tiedot]	[Raportti pdf-muodossa]
TOT 24/94	Kivilouhimossa porari jäi pyöräkuormaajan kauhasta pudotettujen kivilohkareiden alle	[Tarkemmat tiedot]	[Raportti pdf-muodossa]
TOT 7/94	Kaivinkone kaatui hissikuiluun väestönsuojan rakennustyömaalla, kuljettaja putosi 40 metriä kuilun pohjalle	[Tarkemmat tiedot]	[Raportti pdf-muodossa]
TOT 5/94	Trukinkuljettaja ajoi pienoispakettiautolla päin kurottajakuormaajan kauhaa sellutehtaan alueella	[Tarkemmat tiedot]	[Raportti pdf-muodossa]
TOT 28/93	Kuljettajan hukkuminen kaivinkoneen upotessa, kun jäihin vajonnutta traktoria nostettiin käyttämällä kaivinkonetta vetokoneena	[Tarkemmat tiedot]	[Raportti pdf-muodossa]
TOT 21/93	Komu lohcare (n. 5 tonnia) putosi porausvaunun puomeille liukuen niitä pitkin porarin päälle	[Tarkemmat tiedot]	[Raportti pdf-muodossa]
TOT 10/92	Rikastamon käyttömies hautautui holvaantuneen malmimurskeen sortuessa	[Tarkemmat tiedot]	[Raportti pdf-muodossa]

TOT 6/92	Kaivinkoneenkuljettaja hukkui jään pettäessä kaivinkoneen alta	<a href="#">[Tarkemmat tiedot]</a>	<a href="#">[Raportti pdf-muodossa]</a>
TOT 5/91	Murskaamolla sattunut työtapaturma jousipakkaa vaihdettaessa	<a href="#">[Tarkemmat tiedot]</a>	<a href="#">[Raportti pdf-muodossa]</a>
TOT 24/90	Työnjohtaja puristui lohcareiden väliin avolouhoksessa	<a href="#">[Tarkemmat tiedot]</a>	<a href="#">[Raportti pdf-muodossa]</a>
TOT 11/90	Kaivinkoneenkuljettaja hukkui ohjaamoon koneen kaaduttua kyljelleen soramonttuun	<a href="#">[Tarkemmat tiedot]</a>	<a href="#">[Raportti pdf-muodossa]</a>
TOT 35/89	Maansiirtoauton kuljettajan kuolemaan johtanut työtapaturma tämän jäädessä kaivinkoneen kauhassa työskennellessään kannatustukin ja kauhan reunan väliin	<a href="#">[Tarkemmat tiedot]</a>	<a href="#">[Raportti pdf-muodossa]</a>
TOT 5/89	Komun putoaminen kalliotunnelin seinästä porauskoneetta korjaavan porarin päälle	<a href="#">[Tarkemmat tiedot]</a>	<a href="#">[Raportti pdf-muodossa]</a>
TOT 25/88	Työntekijän kuolemaan johtanut työtapaturma hänen poistuttuaan liikkuvasta autosta ja jäätyään hiekka-auton perävaunun alle	<a href="#">[Tarkemmat tiedot]</a>	<a href="#">[Raportti pdf-muodossa]</a>
TOT 9/88	Kuolemaan johtanut työtapaturma jarrujen petettyä ja kuljettajan hypättyä ulos liikkuvasta kauhakuormaajasta ja jäätyä takapyörän alle	<a href="#">[Tarkemmat tiedot]</a>	<a href="#">[Raportti pdf-muodossa]</a>
TOT 46/87	Rakennusapumiehen kuolemaan johtanut työtapaturma rivitalon rakennustyössä.	<a href="#">[Tarkemmat tiedot]</a>	<a href="#">[Raportti pdf-muodossa]</a>
TOT 36/86	Putkimies kulki kaivinkoneen kauhan ja koneen välistä kun kauhassa ollut irtokauha putosi hänen päälleen.	<a href="#">[Tarkemmat tiedot]</a>	<a href="#">[Raportti pdf-muodossa]</a>
TOT 4/86	Kauhakuormaajan kuljettaja menehtyi jäätyään puristuksiin ohjaamoon, kun jäätynyt sorakieleke putosi kuormaajan päälle sorakuopalla.	<a href="#">[Tarkemmat tiedot]</a>	<a href="#">[Raportti pdf-muodossa]</a>
TOT 25/85	Kaivosmies menehtyi jäätyään puristuksiin lastauskoneen kauhan ja liejuvaunun väliin.	<a href="#">[Tarkemmat tiedot]</a>	<a href="#">[Raportti pdf-muodossa]</a>

## Appendix B

The list of associated algorithms for the safety system, together with their respective contents.

Number	Contents	Module
1	Algorithm for Human Presence Detection	PIR Sensor
2	Algorithm for Distance Measurement	Ultrasonic Sensor
3	Algorithm for Acceleration Measurement	Accelerometer
4	Algorithm for Power Supply Monitor	Power Monitor
5	Algorithm for Alarming & Warning System	Alarm system
6	Algorithm for Computing Component Values of Power Monitor Module	Power Monitor

### 1. Algorithm for Human Presence Detection

```
//Define Connection Point:
//Define PIR sensor Connection Pins:
#define pirDigital 3
#define motionLED1 13

//Global Resources:
//Baud rate for Serial Communication:
int baud_rate = 9600;

void setup()
{
    //Starting up the Serial Connection Process:
    Serial.begin(baud_rate);

    //Setting the Connections for PIR sensor:
    pinMode(pirDigital, INPUT);
    pinMode(motionLED1, OUTPUT);
    digitalWrite(motionLED1, LOW);
}

void loop()
{
    //Check the Motion Status in Digital Pin:
    motion();
}

void motion()
{
    int motionStatus = digitalRead(pirDigital);

    if (motionStatus == HIGH)
    {
        digitalWrite(motionLED1, HIGH);
        Serial.println("Motion detected!!!");
    }

    else
    { digitalWrite(motionLED1, LOW);
```



```

        Serial.println("No Motion detected!!!");
    }

```

## 2. Algorithm for Distance Measurement

```

//Define Connection Point:
//Define PIR sensor Connection Pins:
#define pwPin 13
#define triggerPin 12

//Global Resources:
//Baud rate for Serial Communication:
int baud_rate = 9600;

//Stored values for Ultrasonic Sensor:
long pulse, mm;

void setup()
{
    //Starting up the Serial Connection Process:
    Serial.begin(baud_rate);

    //Setting the Connections for Ultrasonic sensor:
    pinMode(pwPin, INPUT);
    pinMode(triggerPin, OUTPUT);
}

void loop()
{
    //Start the Distance Measurement Sequence in Digital Pin:
    start_sensor();
    read_sensor();

    //Print all Distance Values:

    printall();
}

void read_sensor()
{
    pulse = pulseIn(pwPin, HIGH);
    sensor = pulse / 1; //1 pulse (1 uS) is 1mm
}

void start_sensor()
{
    digitalWrite(triggerPin, HIGH);
    delay(1);
    digitalWrite(triggerPin, LOW);
}

```

### 3. Algorithm for Acceleration Measurement

```
//Define Connection Point:
//Define ADXL377 Connection Point:
#define Xaxis A0
#define Yaxis A1
#define Zaxis A2

//Global Resources:
//Baud rate for Serial Communication:
int baud_rate = 9600;

//Accelerometer Configuration:
int scale = 200; //The sensor has +-200g range
int outputVol = 5; //The MCU has 5V maximum output voltage
int lower_limit = 0; //Scaling factor
int upper_limit = (3.3 / outputVol) * 1023;

void setup()
{
    Serial.begin(baud_rate);
}

void loop()
{
    //Read and scale the acceleration values:
    int rawX = analogRead(Xaxis);
    float scaledX = map(rawX, lower_limit, upper_limit, -scale, scale);
    Serial.print("X: ");
    Serial.print(scaledX);
    Serial.println(" g");

    int rawY = analogRead(Yaxis);
    float scaledY = map(rawY, lower_limit, upper_limit, -scale, scale);
    Serial.print("Y: ");
    Serial.print(scaledY);
    Serial.println(" g");

    int rawZ = analogRead(Zaxis);
    float scaledZ = map(rawZ, lower_limit, upper_limit, -scale, scale);
    Serial.print("Z: ");
    Serial.print(scaledZ);
    Serial.println(" g");

    delay(2000);
}
```

#### 4. Algorithm for Power Monitor

```
//Define Connection Point:
// Define Battery Monitor Connection Pins:
#define batteryLevel A3
#define batteryPulse 5

//Global Resources
//Baud rate for Serial Communication;
int baud_rate = 9600;

//Reference Voltage
int AREF = 4.096; //Real values from AREF is 4.096V (from Shunt Diode)

void setup()
{
    //Starting up the Serial Connection Process:
    Serial.begin(baud_rate);

    //Battery Monitor:
    pinMode(batteryLevel, INPUT);
    pinMode(batteryPulse, OUTPUT);
    digitalWrite(batteryPulse, LOW);
}

void loop()
{
    battery();
}

void battery()
{
    //Enable the Gate-Control Pulse from MCU:
    digitalWrite(batteryPulse, HIGH);
    delayMicroseconds(2);
    digitalWrite(batteryPulse, LOW);
    delayMicroseconds(2);

    //Read the current battery level:
    float batteryValue = analogRead(batteryLevel);
    double batteryVoltage = (double)batteryValue / 1023 * AREF;

    //Perform the battery level check:
    if (batteryVoltage >= 4.5)
    {
        Serial.println("Battery Level: Sufficient!!!");
    }

    else if ((batteryVoltage <= 4.5) || (batteryVoltage >= 2.25))
    {
        Serial.println("Battery Level: Low!!!");
    }

    else if (batteryVoltage < 2.25)
    {
        Serial.println("Battery Level: CRITICAL LOW!!!");}
}
```

## Appendix C

Connection guides, and the communication protocol setup guide for the Arduino microcontrollers in the first and the second prototypes.

Table i: Connection Guide for the Arduino microcontroller in the first prototype.

Components	Pin	Connection to Arduino
Ultrasonic Sensor HC SR04	+5V	+5V
	Trigger	12
	Echo	11
	GND	GND
Alarm system (Buzzer + LED)	(Buzzer) V+	7
	(Buzzer) GND	GND
	(Safe LED) V+	8
	(Safe LED) GND	GND
	(Warning LED) V+	5
	(Warning LED) GND	GND

Table ii: Communication Protocol setup in the second prototype.

XBee Transmitter	Channel (CH)	C
	Pan ID (ID)	1001
	Coordinator Enable (CE)	Coordinator
	Baud rate	9600
XBee Receiver	Channel (CH)	C
	Pan ID (ID)	1001
	Coordinator Enable (CE)	Endpoint
	Baud rate	9600

Table iii: Connection Guide for the Arduino microcontroller on the Transceiver side in the second prototype.

Components	Pin	Connection to Arduino
Ultrasonic Sensor HRLV-MaxSonar EZ1	+5V	+5V
	GND	GND
	Digital Output	13
Alarm system (Buzzer + LED+LCD)	(Buzzer) V+	4
	(Buzzer) GND	GND
	(Safe LED) V+	3
	(Safe LED) GND	GND
	(Warning LED) V+	2
	(Warning LED) GND	GND
Open PIR Sensor	V+	+5V
	GND	GND
	Digital Output	12
Accelerometer	+5V	+5V
	GND	GND
	X-axis Output	A5
	Y-axis Output	A4
	Z-axis Output	A3
XBee Module	+5V	+5V
	GND	GND
	Dout	0 (Rx)
	Din	1 (Tx)

Table iv: Connection Guide for the Arduino microcontroller on the Receiver side in the second prototype.

Components	Pin	Connection to Arduino
Alarm system (Buzzer + LED+LCD)	(Buzzer) V+	7
	(Buzzer) GND	GND
	(Safe LED) V+	8
	(Safe LED) GND	GND
	(Warning LED) V+	5
	(Warning LED) GND	GND
XBee Module	+5V	+5V
	GND	GND
	Dout	0 (Rx)
	Din	1 (Tx)

